NATIONAL ADVISORY COMMITTEE FOR AERONAUTICS

TECHNICAL NOTE 2467

THE AERODYNAMIC BEHAVIOR OF A HARMONICALLY OSCILLATING FINITE SWEPTBACK WING IN SUPERSONIC FLOW

By Chieh-Chien Chang

The Johns Hopkins University

Washington

October 1951

NATIONAL ADVISORY COMMITTEE FOR AERONAUTICS

TECHNICAL NOTE 2467

THE AERODYNAMIC BEHAVIOR OF A HARMONICALLY OSCILLATING FINITE SWEPTBACK WING IN SUPERSONIC FLOW

By Chieh-Chien Chang

SUMMARY

By an extension of Evvard's "diaphragm" concept outside the wing tip, the present paper presents two approximate methods for calculating the aerodynamic behavior of harmonically oscillating, sweptback finite wings with both supersonic leading and trailing edges. Both methods are based upon the fact that the contribution of the so-called "diaphragm" on the potential at a fixed point on the wing is approximately canceled by the contribution of a portion of the wing itself, if the wing undergoes steady harmonic oscillation at a low value of the frequency parameter $\frac{\omega c}{a\beta^2}$ (where ω is angular velocity per second; c is chord; a is velocity of sound; and $\beta = \sqrt{M^2 - 1}$, M being Mach number). It is further necessary that the point be influenced by the diaphragm from only one wing tip.

The first method expresses the integration in terms of Fresnal integrals. The final expressions for the pressure coefficient are in the form of integrals which may be readily evaluated, using numerical integration with available mathematical tables. Some calculations are shown, and the results check well with the results of the second method. It is expected that this method should give accurate results in the engineering sense if the frequency parameter $\frac{\omega c}{a\beta^2}$ is of the order one-half or less. Even if the frequency parameter exceeds this value, the pressure increments calculated asymptotically approach the correct values at the inner edges of the tip Mach cone.

As a byproduct of the above approach, the expressions for the downwash of the wing wake, influenced by only the two tip diaphragms, are given in terms of Fresnal integrals.

The second method is similar to the first one except that a series expansion of the source-strength function is used. When the frequency parameter is small $\left(\frac{\omega c}{a\beta^2} < \frac{1}{2}\right)$, the few terms used give good engineering

accuracy. In the present case, five terms are considered. Of course, the number of terms must increase as the frequency parameter increases. This method gives closed expressions for the pressure coefficients. In applying the method, the calculations are lengthy, but no great computing skill is required. For the benefit of design engineers, some expressions of the average pressure coefficient over the entire rectangular wing tip influenced by three-dimensional flow are given in a closed form, so that they can be used to estimate the tip effect in preliminary design.

A number of graphs are presented to show the pressure distribution of the wings at different Mach numbers, sweepback angles, and frequency parameters. Comparisons of the pressure coefficients calculated from the present methods and the exact two-dimensional solutions based on linearized theory are made.

INTRODUCTION

The aerodynamic behavior of a harmonically oscillating finite wing in a supersonic flow has been recently studied by a number of investigators, particularly Garrick and Rubinow (reference 1), Evvard (reference 2), and Miles (reference 3). From the viewpoint of mathematical physics, it is one phase of the mechanics of wave motion investigated by a number of great physicists and applied mathematicians such as Huyghens (reference 4), Maxwell, Kirchhoff, Sommerfeld, Hadamard, Volterra, and others over a number of years. The classical treatment, however, is principally along the line of Cauchy's initial-value problem, while the present aerodynamic problem is a boundary-value problem. The classical results are of some help in the formulation of the present problem but not of much help in the solution.

With the advent of guided missiles and aircraft operating in the supersonic range, trouble has been experienced with flutter of the wing or control systems. It was such troubles that spurred the author to obtain an understanding of the aerodynamic behavior of a harmonically oscillating finite wing at supersonic speed. The two-dimensional case of an arbitrary unsteady motion has been solved in the last few years (references 5, 6, 7, and 8). But in the three-dimensional case up to now very few useful results have been achieved.

The present paper treats the case of a finite wing with the leading edge ahead of the Mach line. The wing may be swept back or forward. Another condition has to be imposed, that the Mach cones at the nose and the tip never intersect within the wing area. With slight modification, the method can be extended to more general wing plan forms. The wing is supposed to undergo harmonic oscillations of small amplitude during flight at supersonic speed.

For the wing plan form as specified above, the three-dimensional flow fields are limited to three portions of the wing area: the area within the nose Mach cone, and the two areas within the tip Mach cones. In the remaining wing areas, the aerodynamic behavior can be calculated with the two-dimensional theory of swept wings with supersonic leading and trailing edges under harmonic oscillation (reference 6, e.g.). Therefore, the present investigation is limited to the tip area and nose area of the wing.

The author should express his appreciation to Miss V. O'Brien, Miss P. Clarken, and Mr. B. T. Chu for their assistance in carrying out the project. The present project was conducted at The Johns Hopkins University under the sponsorship and with the financial assistance of the National Advisory Committee for Aeronautics.

LINEARIZED DIFFERENTIAL EQUATION AND SOLUTIONS OF SOURCE INTEGRATION

General Analysis

The linearized differential equation of unsteady compressible flow is well-known (references 1 and 5)

$$\frac{\partial^2 \phi}{\partial x^2} + \frac{\partial^2 \phi}{\partial y^2} + \frac{\partial^2 \phi}{\partial z^2} = \frac{1}{a^2}\left(\frac{\partial}{\partial t} + U\frac{\partial}{\partial x}\right)^2 \phi \tag{1a}$$

or, briefly,

$$\nabla^2 \phi = \frac{1}{a^2}\left(\frac{\partial}{\partial t} + U\frac{\partial}{\partial x}\right)^2 \phi \tag{1b}$$

where U is the free-stream velocity and a is the sound speed of the free-stream condition. (Symbols used in this paper are defined in appendix A.) The velocity vector $\bar{q} = U\bar{i} + \bar{q}' = U\bar{i} + \text{grad}\ \phi$ and ∇^2 is the Laplacian operator. The elementary solution of the potential at a point (x,y,z) at time t due to a source of time-dependent strength A is

$$\phi_o(x,y,z,t;\ \xi,\eta,\zeta) = \frac{A(\xi,\eta,\zeta,t - \tau_1) + A(\xi,\eta,\zeta,t - \tau_2)}{r} \tag{2a}$$

where the source is located at (ξ,η,ζ) and

$$r = \frac{1}{\beta^2}\sqrt{(x - \xi)^2 - \beta^2\left[(y - \eta)^2 + (z - \zeta)^2\right]} \tag{3}$$

$$\left.\begin{aligned} \tau_1 &= \frac{(x - \xi)M}{a\beta^2} - \frac{r}{a} \\ \tau_2 &= \frac{(x - \xi)M}{a\beta^2} + \frac{r}{a} \end{aligned}\right\} \tag{4}$$

where

$$\beta^2 = M^2 - 1$$

In the case of harmonically oscillating source strength the source-strength function can be written as a product of two functions, one containing the source position and the other showing the time dependence, or, explicitly,

$$A(\xi,\eta,\zeta,t - \tau) = \bar{A}(\xi,\eta,\zeta)f(t - \tau)$$

Equation (2a) then becomes:

$$\phi_o(x,y,z,t;\ \xi,\eta,\zeta) = \frac{\bar{A}(\xi,\eta,\zeta)}{r}\left[f\left(t - \tau_1\right) + f\left(t - \tau_2\right)\right] \tag{2b}$$

In the whole domain surrounding the wing in supersonic flight, there is one particular streamline surface which is of interest to the problem. This streamline surface is formed by the streamlines, which coming from upstream either strike the wing leading edge or pass through the foremost Mach line of the tip Mach cones. It follows the contour of the wing (both upper and lower surfaces), reunites at the trailing edge, and then extends to infinity at downstream.

Figure 1 shows the streamline surface which is associated with an oscillating wing in a supersonic flow at time t.

The whole streamline surface can be divided into eight zones as shown. Ahead of the supersonic leading edge and outside the two tip Mach cones, the flow is not influenced by any of the disturbances caused by the wing. This is called zone 1 as shown. The portion of the streamline surface behind the supersonic leading edge and between the tip Mach cones is called zone 2. In this zone the potential at any point on the top wing surface (or bottom) is never influenced by the flow on the opposite side. Therefore, the source solution of equation (2b) can be applied without restriction, if the source-strength function A is known.

Zone 3 represents the portion of the wing influenced by the right tip Mach cone and zone 4 by the left tip Mach cone. In these two zones, the flow on one wing surface is influenced by the flow on the opposite side. The simple source solution of equation (2b) cannot be applied. The present paper gives the approximate solution for these two zones for the case where the two tip Mach cones meet on or outside the trailing edge. The present method with slight modification can also be extended to the case that the tip Mach cones intersect inside the wing area (not shown in fig. 1), but no diaphragm within the forward Mach cone of the point under consideration is influenced by the diaphragm on the other side.

Zone 5 is the portion of the streamline surface outside the wing surface influenced only by the right tip Mach cone; similarly zone 6 is influenced only by the left tip Mach cone. Zone 7 is the portion of the streamline surface after the trailing edge influenced by neither Mach cone. Zone 8 is the portion of the streamline surface influenced by both Mach cones. Of course, if the wing moves slightly up and down with time, the streamline surface and consequently the diaphragm must also move up and down with it. With the concept of Evvard (reference 9), any finite wing in supersonic flow can be considered to be attached over its streamline surface outside the wing (such as zones 5, 6, 7, and 8) to a thin weightless rubber diaphragm, of which the pressure on both sides at a point must be balanced and through which no fluid can leak.

The diaphragm is imagined to extend to the outer edge of the tip Mach cone, and to coincide with the shape of the streamline surface. Thus, the rubber diaphragm can be considered as an extension of the wing. The flow on the upper side of the wing with its extension can be considered as independent of the flow on the lower side of the wing and vice versa. The potential at any point on one side of the wing can be evaluated from the source distribution on the same side of the wing and the diaphragm within the forward Mach cone of that point. In the steady case it has been shown by Puckett that the source strength at a point

of the wing is directly proportional to the slope at the point and independent of the slope of its neighboring points. Evvard has shown that the solutions obtained using the diaphragm concept are identical to those of conical flow (reference 9).

For steady flows, the principal advantage of Evvard's method is that the slope of a point on the diaphragm is determined solely by the slopes of the wing surface along the characteristic or Mach line through the point, as long as the point on the diaphragm is ahead of the Mach cone from the other wing tip. In the case of unsteady flow, it can be shown that the above statement is approximately true if the wing slopes vary very slowly with time. Using the diaphragm concept, the disturbance potential at any point can be considered as the effect of sources of the wing system on the same side. (Of course, the slope of the imaginary diaphragm depends on the flows over both wing surfaces.) It becomes apparent that the potential can be evaluated by the well-known source-integration method. Let us consider a point on the diaphragm where the potential contributed by sources on either side of the wing must be the same. It has been shown by Evvard that the source strength is proportional to the vertical component of the perturbation velocity, or, more directly, is proportional to the local slope of the wing surface or the diaphragm even if the flow is not steady. Mathematically, this is shown as $A = \frac{w}{\pi\beta^2} = \frac{U\alpha}{\pi\beta^2}$ where w is the vertical component of the perturbation velocity and α denotes the slope of the streamline surface.

The following equations can be written to denote:

The slope at the upper wing surface at time $t - \tau_1$ by

$$\sigma_{T,1} = \sigma_T(\xi,\eta,+0,t - \tau_1)$$

The slope of the upper wing surface at time $t - \tau_2$ by

$$\sigma_{T,2} = \sigma_T(\xi,\eta,+0,t - \tau_2)$$

The slope of the lower wing surface at time $t - \tau_1$ by

$$\sigma_{B,1} = \sigma_B(\xi,\eta,-0,t - \tau_1)$$

The slope of the lower wing surface at time $t - \tau_2$ by

$$\sigma_{B,2} = \sigma_B(\xi,\eta,-0,t - \tau_2)$$

The slope on the diaphragm at time $t - \tau_1$ by

$$\lambda_1 = \lambda(\xi,\eta,0,t - \tau_1)$$

The slope on the diaphragm at time $t - \tau_2$ by

$$\lambda_2 = \lambda(\xi,\eta,0,t - \tau_2)$$

(5)

Then the potential can be written at any point on the top or bottom streamline surface as:

$$\left.\begin{aligned}
\phi_T(x,y,+0,t) &= -\frac{U}{2\pi\beta^2}\iint_{S_w}\frac{\left(\sigma_{T,1}+\sigma_{T,2}\right)\,d\xi\,d\eta}{r} - \\
&\quad \frac{U}{2\pi\beta^2}\iint_{S_D}\frac{\left(\lambda_1+\lambda_2\right)\,d\xi\,d\eta}{r} \\
\phi_B(x,y,-0,t) &= -\frac{U}{2\pi\beta^2}\iint_{S_w}\frac{\left(\sigma_{B,1}+\sigma_{B,2}\right)\,d\xi\,d\eta}{r} - \\
&\quad \frac{U}{2\pi\beta^2}\iint_{S_D}\frac{\left(\lambda_1+\lambda_2\right)\,d\xi\,d\eta}{r}
\end{aligned}\right\} \qquad (6)$$

Or, in an oblique coordinate system whose axes lie parallel to the Mach lines and whose origin is placed at the point of tangency of the Mach line to the leading edge of the wing tip (the junction of the supersonic and subsonic leading edge) (see fig. 2), these equations can be written as:

$$\left.\begin{aligned}
\phi_T(u,v,+0,t) = &-\frac{U}{2\pi M}\iint_{S_{w1}+S_{w2}} \frac{\sigma_T(u',v',t-\tau_1)+\sigma_T(u',v',t-\tau_2)}{\sqrt{(u-u')(v-v')}}\,du'\,dv' - \\
&\frac{U}{2\pi M}\iint_{S_D} \frac{\lambda(u',v',t-\tau_1)+\lambda(u',v',t-\tau_2)}{\sqrt{(u-u')(v-v')}}\,du'\,dv' \\
\phi_B(u,v,-0,t) = &-\frac{U}{2\pi M}\iint_{S_{w1}+S_{w2}} \frac{\sigma_B(u',v',t-\tau_1)+\sigma_B(u',v',t-\tau_2)}{\sqrt{(u-u')(v-v')}}\,du'\,dv' - \\
&\frac{U}{2\pi M}\iint_{S_D} \frac{\lambda(u',v',t-\tau_1)+\lambda(u',v',t-\tau_2)}{\sqrt{(u-u')(v-v')}}\,du'\,dv'
\end{aligned}\right\} \tag{7}$$

where (u,v) is the transformed coordinate of the point originally at (x,y) and (u',v') is the transformed coordinate of the source element originally at (ξ,η) in the x,y system. The old and new coordinate systems are related by the following transformation equations:

$$\left.\begin{aligned}
u &= \frac{M}{2\beta}(x-\beta y) & v &= \frac{M}{2\beta}(x+\beta y) \\
x &= \frac{\beta}{M}(v+u) & y &= \frac{1}{M}(v-u) \\
u' &= \frac{M}{2\beta}(\xi-\beta\eta) & v' &= \frac{M}{2\beta}(\xi+\beta\eta) \\
\xi' &= \frac{\beta}{M}(v'+u') & \eta &= \frac{\beta}{M}(v'-u') \\
d\xi\,d\eta &= \frac{2\beta}{M^2}\,du'\,dv'
\end{aligned}\right\} \tag{8a}$$

and the quantity r and the time intervals τ_1 and τ_2 in the new coordinate system are, respectively:

$$\left.\begin{aligned} r &= \frac{2}{M\beta}\sqrt{(u-u')(v-v')} \\ \tau_1 &= \frac{1}{a\beta}(v-v'+u-u') - \frac{2}{a\beta M}\sqrt{(u-u')(v-v')} \\ \tau_2 &= \frac{1}{a\beta}(v-v'+u-u') + \frac{2}{a\beta M}\sqrt{(u-u')(v-v')} \end{aligned}\right\} \tag{8b}$$

If the supersonic and subsonic leading edges are denoted by the equation (see figs. 2, 3, and 4)

$$\left.\begin{aligned} v &= v_1(u) \quad \text{or} \quad u = u_1(v) \\ v &= v_2(u) \quad \text{or} \quad u = u_2(v) \end{aligned}\right\} \tag{9}$$

then the potential at any point (u_w, v_w) on the wing can be written as:

$$\begin{aligned} \phi_T(u_w, v_w, +0, t) = &-\frac{U}{2\pi M}\int_{u_2(v_w)}^{u_w} \frac{du'}{(u_w-u')^{1/2}} \int_{v_1(u')}^{v_w} \frac{\sigma_T(u',v',t-\tau_1) + \sigma_T(u',v',t-\tau_2)}{(v_w-v')^{1/2}}\,dv' - \\ &\frac{U}{2\pi M}\int_0^{u_2(v_w)} \frac{du'}{(u_w-u')^{1/2}}\left[\int_{v_1(u')}^{v_2(u')} \frac{\sigma_T(u',v',t-\tau_1) + \sigma_T(u',v',t-\tau_2)}{(v_w-v')^{1/2}}\,dv' + \right. \\ &\left.\int_{v_2(u')}^{v_w} \frac{\lambda(u',v',t-\tau_1) + \lambda(u',v',t-\tau_2)}{(v_w-v')^{1/2}}\,dv'\right] \end{aligned} \tag{10}$$

(A similar expression can be obtained for ϕ_B.) Now it will be shown that in the case of harmonic oscillation the second integral is approximately zero under certain conditions.

For steady harmonic oscillation of a thin flat wing, assume:

$$-\sigma_B = \sigma_T = \alpha = \bar{\alpha}e^{i\omega t} \tag{11a}$$

where $\bar{\alpha}$ is everywhere the same on the wing.

Further, assume:

$$\lambda = \bar{\lambda}(u,v)e^{i\omega t} \tag{11b}$$

where $\bar{\lambda}(u,v)$ is the amplitude of oscillation of points on the diaphragm and is a function of the point (u,v). The term $\bar{\lambda}(u,v)$ may be complex, including the time lag of the oscillation, because the time lag must be a function of location only.

With σ and λ given by equations (11a) and (11b), respectively, the second integral (along constant u) of equation (10) can be written as:

$$\int_{v_1(u')}^{v_2(u')} \frac{\sigma_T\left(u',v',t-\tau_1\right)+\sigma_T\left(u',v',t-\tau_2\right)}{(v_w-v')^{1/2}}\,dv' + \int_{v_2(u')}^{v_w} \frac{\lambda\left(u',v',t-\tau_1\right)+\lambda\left(u',v',t-\tau_2\right)}{(v_w-v')^{1/2}}\,dv' =$$

$$2e^{i\omega\left[t-\frac{1}{a\beta}(u_w-u')\right]}\left\{\bar{\alpha}\int_{v_1(u')}^{v_2(u')} \frac{e^{\frac{-i\omega}{a\beta}(v_w-v')}\cos\left[\frac{2\omega}{a\beta M}(u_w-u')^{1/2}(v_w-v')^{1/2}\right]}{(v_w-v')^{1/2}}\,dv' + \right.$$

$$\left.\int_{v_2(u')}^{v_w} \frac{\bar{\lambda}(u',v')e^{\frac{-i\omega}{a\beta}(v_w-v')}\cos\left[\frac{2\omega}{a\beta M}(u_w-u')^{1/2}(v_w-v')^{1/2}\right]}{(v_w-v')^{1/2}}\,dv'\right\} \tag{12}$$

When $\omega = 0$, that is, the steady case, this integral reduces to Evvard's result in reference 2 and has been shown to be exactly zero. For $\omega \neq 0$, the integral will again be zero if $\cos\left[\frac{2\omega}{a\beta M}(u_w - u')^{1/2}(v_w - v')^{1/2}\right] = 1$ exactly. This will be clear from the following consideration.

Evvard in reference 2, equation (24), showed that for any point (u_D, v_D) on the diaphragm (see fig. 2) the following relation exists along the characteristics line $u' = u_D$:

$$\int_{v_2(u')}^{v_D} \frac{\lambda(u',v',t - \tau_1) + \lambda(u',v',t - \tau_2)}{(v_D - v')^{1/2}}\,dv' =$$

$$\int_{v_1(u')}^{v_2(u')} \frac{\sigma_B(u',v',t - \tau_1) + \sigma_B(u',v',t - \tau_2) - \sigma_T(u',v',t - \tau_1) - \sigma_T(u',v',t - \tau_2)}{2(v_D - v')^{1/2}}\,dv' \quad (13)^1$$

This means that along the characteristic line u = Constant the total effect of the diaphragm source strength is equal to the total effect of source strength on both wing surfaces along the same characteristics, and that it is independent of the source strength of the diaphragm or the wing surface outside the above characteristics. Now, along this element $u' = u_D$,

---

[1]Members of the NACA staff recently expressed the opinion that "Since τ_1 and τ_2 contain the variables u', a second-order integral equation is generally required rather than the simplified first-order integral equation given. Equation [13] is satisfactory if τ may be represented as varying linearly with time in the interval $(\tau_1 - \tau_2)$." In the present analysis, the use of equation (13) is justified.

$$\tau_1 = \frac{1}{a\beta}\left(v_D - v'\right) = \tau_2$$

Substituting equations (11a), (11b), and the above value of the τ's into equation (13), there is obtained:

$$\int_{v_2(u')}^{v_D} \frac{\bar{\lambda}(u',v')e^{i\omega\left(t - \frac{v_D - v'}{a\beta}\right)}}{\left(v_D - v'\right)^{1/2}}\,dv' = -\int_{v_1(u')}^{v_2(u')} \frac{\bar{\alpha}e^{i\omega\left(t - \frac{v_D - v'}{a\beta}\right)}}{\left(v_D - v'\right)^{1/2}}\,dv' \qquad (14)$$

Now if in equation (12) $\cos\left[\frac{2\omega}{a\beta M}\left(u_w - u'\right)^{1/2}\left(v_w - v'\right)^{1/2}\right] = 1$ exactly, the integral at the right-hand side of the equation will reduce to the form:

$$\bar{\alpha}\int_{v_1(u')}^{v_2(u')} \frac{e^{\frac{-i\omega}{a\beta}\left(v_w - v'\right)}}{\left(v_w - v'\right)^{1/2}}\,dv' + \int_{v_2(u')}^{v_w} \frac{\bar{\lambda}(u',v')e^{\frac{-i\omega}{a\beta}\left(v_w - v'\right)}}{\left(v_w - v'\right)^{1/2}}\,dv' \qquad (15)$$

which according to equation (14) is zero, because here $v_w = v_D$.

In general, $\cos\left[\frac{2\omega}{a\beta M}\left(u_w - u'\right)^{1/2}\left(v_w - v'\right)^{1/2}\right] = \cos\frac{\omega r}{a}$ is less than unity. (Note that $r = \frac{1}{\beta^2}\sqrt{(x - \xi)^2 - \beta^2(y - \eta)^2}$ is the hyperbolic distance, not the geometrical distance.) But for small values of $\frac{\omega r}{a}$, the variation of $\cos\frac{\omega r}{a}$ from unity is very small. Suppose that the following condition is imposed: $\frac{\omega r}{a} \leq \frac{1}{2}$. Then $1 \geqq \cos\frac{\omega r}{a} \geqq 1 - \frac{1}{2}\left(\frac{\omega r}{a}\right)^2 = 0.875$. In both integrals the factor $\cos\frac{\omega r}{a}$ will reduce the value of each integrand a small percentage in view of the monotonically decreasing nature of $\cos\frac{\omega r}{a}$ for small values of $\frac{\omega r}{a}$. Of course, the net contribution of both integrals cannot cancel out exactly as if $\cos\frac{\omega r}{a} = 1$, which is located on the left tip Mach line.

For a first approximation, however, there can be written that the contribution of the diaphragm S_D (fig. 2) and the portion of wing area S_{w2} cancel each other; otherwise, the solution is too difficult to obtain, particularly with sweptback wings. Equation (10) will then become:

$$\phi_T(u_w, v_w, +0, t) = -\frac{U}{2\pi M} \int_{v_2(u_w)}^{u_w} \frac{du'}{(u_w - u')^{1/2}} \int_{v_1(u')}^{v_w} \frac{\sigma_T(u', v', t - \tau_1) + \sigma_T(u', v', t - \tau_2)}{(v_w - v')^{1/2}} dv' \quad (16)$$

If the above approximation is analyzed more carefully, it will be found that the average value of $\cos \frac{\omega r}{a}$ on the diaphragm is slightly larger than that on the wing. This can be shown in the following way: On the diaphragm $v_2 \leqq v' \leqq v_w$, and on the wing $v_1 \leqq v' \leqq v_2$ (fig. 2). For the purpose of illustration, take the average value of $v' = \frac{v_w + v_2}{2}$ on the diaphragm and $v' = \frac{v_1 + v_2}{2}$ on the wing. Then it is clear that

$$\left\{\cos\left[\frac{2\omega}{a\beta M}(u_w - u')^{1/2}\left(v_w - \frac{v_1 + v_2}{2}\right)^{1/2}\right]\right\}_w \leqq \left\{\cos\left[\frac{2\omega}{a\beta M}(u_w - u')^{1/2}\left(\frac{v_w - v_2}{2}\right)^{1/2}\right]\right\}_D$$

if $\frac{\omega r}{a} < \frac{1}{2}$. In other words, the contribution of the diaphragm is slightly more than the opposite contribution of the wing area S_{w2} to the tip corner of the trailing edge, particularly on the side edge of the tip where the contribution due to the wing area S_{w1} is zero (see equation (16) and fig. 3). Therefore, the pressure at the side edge of the tip cannot be zero as predicted with the present approximation. But as the point considered approaches the left

characteristic of the right Mach cone (i.e., r = 0) the present approximation approaches the exact solution as a limit. This is favorable to the present approximation for two reasons. First, the pressure increment in the neighborhood of the side edge of the tip is expected to be negligibly small, particularly at a low frequency parameter. Its contribution to the aerodynamic behavior of the wing specified is negligible. The present approximation asymptotically approaches the exact value near the left tip Mach line where the magnitude of pressure increment is much higher and becomes more important to the aerodynamic behavior of the wing than that at the side edge of the tip. Besides, the major portion of the wing area is calculated by the two-dimensional theory as shown in references 5 and 6 and total contribution of the tip is usually not too important. Therefore, the approximation is of good engineering accuracy.

Calculation of Downwash Angle $\lambda\left(u,v_D,t\right)$ for Harmonically Oscillating Wing

In reference 2 (equation (26)), Evvard has shown that the downwash angle in zone 5 or 6 (fig. 1) is given by:

$$\lambda\left(u,v_D,t\right) = \frac{1}{2\pi\left(v_D - v_2\right)^{1/2}} \int_{v_1(u)}^{v_2(u)} \frac{\left[\sigma_B\left(u,v',t - \frac{v_D - v'}{a\beta}\right) - \sigma_T\left(u,v',t - \frac{v_D - v'}{a\beta}\right)\right]\left(v_2 - v'\right)^{1/2}}{\left(v_D - v'\right)^{1/2}} dv' \tag{17}$$

[2]

An approximate method of evaluating the above integral is presented below.

If equation (11a) is substituted into equation (17), the following equation is obtained:

$$\lambda\left(u,v_D,t\right) = -\frac{\bar{\alpha}e^{i\omega t}}{\pi\left(v_D - v_2\right)^{1/2}} \int_{v_1(u)}^{v_2(u)} \frac{e^{\frac{-i\omega}{a\beta}\left(v_D - v'\right)}}{\left(v_D - v_1'\right)^{1/2}} \left(v_2 - v'\right)^{1/2} dv' \tag{18}$$

[2]See remarks about equation (13).

Obviously,

$$\lambda \longrightarrow \infty \quad \text{as} \quad v_D \longrightarrow v_2$$

$$\lambda \longrightarrow 0 \quad \text{as} \quad v_D \longrightarrow \infty$$

For the case $v_D > v_2$ (fig. 2), $v_2 - v_1$ can be divided into n equal parts and the ith division can be denoted by v_i' (where $v_i' = v_1$ for $i = 0$ and $v_i' = v_2$ for $i = n$). Then,

$$\lambda\left(u, v_D, t\right) = -\frac{\bar{\alpha} e^{i\omega t}}{\pi\left(v_D - v_2\right)^{1/2}} \sum_{i=0}^{n} \int_{v_i'}^{v_i'+1} \frac{e^{\frac{-i\omega}{a\beta}\left(v_D - v'\right)}}{\left(v_D - v'\right)^{1/2}} \left(v_2 - v'\right)^{1/2} dv'$$

$$= -\frac{\bar{\alpha} e^{i\omega t}}{\pi\left(v_D - v_2\right)^{1/2}} \sum_{i=0}^{n} \left(v_2 - v'\right)^{1/2} \int_{v_i'}^{v_i'+1} \frac{e^{\frac{-i\omega}{a\beta}\left(v_D - v'\right)}}{\left(v_D - v'\right)^{1/2}} dv' \tag{19}$$

where the division is so fine that $v_2 - v' = v_2 - v_i'$ can be taken out of the integration sign for the first approximation. Incidentally, the integral left can be transformed to the Fresnal integral (reference 10). Equation (19) then becomes:

$$\lambda\left(u, v_D, t\right) = \left(\frac{2a\beta}{\pi\omega}\right)^{1/2} \frac{\bar{\alpha} e^{i\omega t}}{\left(v_D - v_2\right)^{1/2}} \sum_{i=0}^{n} \left(v_2 - v_i\right)^{1/2} \left[C\left(Z_{i+1}\right) - C\left(Z_i\right) - iS\left(Z_{i+1}\right) + iS\left(Z_i\right)\right] \tag{20}$$

where

$$\left.\begin{aligned} Z_i &= \left(\frac{2\omega}{a\beta\pi}\right)^{1/2}\left(v_D - v_i\right)^{1/2} \\ C(Z) &= \int_0^Z \cos\frac{\pi}{2}Z^2\,dZ \\ S(Z) &= \int_0^Z \sin\frac{\pi}{2}Z^2\,dZ \end{aligned}\right\} \qquad (21)$$

Some of the basic properties of the Fresnal integral are given in equations (29).

APPROXIMATION THEORY OF VELOCITY POTENTIAL AND PRESSURE COEFFICIENT AT A POINT ON A HARMONICALLY OSCILLATING SWEPTBACK FINITE WING WITH SUPERSONIC LEADING EDGE[3] - FIRST METHOD

Assume the whole wing flapping up and down according to $\sigma_T(t) = \bar{\alpha}e^{i\omega t}$ where $\bar{\alpha}$ is the amplitude of oscillation. In fact,

$$\bar{\alpha} = \frac{\text{Maximum descending rate of wing } \dot{h}_{max}}{\text{Free-stream velocity } U}$$

The frequency of oscillation per second is $\frac{\omega}{2\pi}$. The velocity potential of such oscillation may be considered as due to harmonic sources and is

[3]The author should express his appreciation to Dr. J. C. Evvard for a discussion on this approximation method in May 1948.

given by equation (6). It has also been shown that for the harmonically oscillating wing, equation (6) can be further simplified to equation (16) as follows:

$$\phi_T(u_w, v_w, +0, t) = -\frac{U\bar{\alpha}e^{i\omega t}}{2\pi\beta^2} \iint_{S_{wl}} \frac{e^{-i\omega\tau_1} + e^{-i\omega\tau_2}}{r} \, d\xi \, d\eta$$

$$= -\frac{U}{2\pi M} \int_{v_2(u_w)}^{u_w} \frac{du'}{(u_w - u')^{1/2}} \int_{v_1(u)}^{v_w} \frac{\sigma_T(u', v', t - \tau_1) + \sigma_T(u', v', t - \tau_2)}{(v_w - v')^{1/2}} \, dv' \quad (22a)$$

where

$$\sigma_T(u', v', t - \tau_1) = \bar{\alpha}e^{i\omega(t-\tau_1)} = \bar{\alpha}e^{i\omega\left[t - \frac{1}{a\beta}(v_w - v' + u_w - u') + \frac{2}{a\beta M}(u_w - u')^{1/2}(v_w - v')^{1/2}\right]}$$

$$\sigma_T(u', v', t - \tau_2) = \bar{\alpha}e^{i\omega(t-\tau_2)} = \bar{\alpha}e^{i\omega\left[t - \frac{1}{a\beta}(v_w - v' + u_w - u') - \frac{2}{a\beta M}(u_w - u')^{1/2}(v_w - v')^{1/2}\right]}$$

Since in most practical cases straight leading edges are under consideration, put (cf. equation (9) and fig. 3):

$$v = v_1(u) = k_1 u \quad \text{or} \quad u = u_1(v) = v/k_1$$

$$v = v_2(u) = k_2 u \quad \text{or} \quad u = u_2(v) = v/k_2$$

as the equation of the supersonic wing edge outside the tip Mach cone and the subsonic leading edge within the Mach cone. Then, equation (22a) can be written as:

$$\phi(u_w, v_w, +0, t) = -\frac{U\sigma e^{i\omega t}}{2M\pi} \int_{v_w/k_2}^{u_w} \frac{du'}{(u_w - u')^{1/2}} \int_{k_1 u}^{v_w} \frac{dv'}{(v_w - v')^{1/2}} e^{\frac{-i\omega}{a\beta}\left[(v_w - v' + u_w - u') \mp \frac{2}{M}(u_w - u')^{1/2}(v_w - v')^{1/2}\right]} \tag{22b}$$

where it is understood that $e^{\frac{-i\omega}{a\beta}\left[(v_w - v' + u_w - u') \mp \frac{2}{M}(u_w - u')^{1/2}(v_w - v')^{1/2}\right]}$ stands for the sum of $e^{\frac{-i\omega}{a\beta}\left[(v_w - v' + u_w - u') - \frac{2}{M}(u_w - u')^{1/2}(v_w - v')^{1/2}\right]}$ and $e^{\frac{-i\omega}{a\beta}\left[(v_w - v' + u_w - u') + \frac{2}{M}(u_w - u')^{1/2}(v_w - v')^{1/2}\right]}$

Introducing the following new variables Z and $\overline{Z}$ instead of v',

$$Z = \left(\frac{2\omega}{a\beta\pi}\right)^{1/2}\left[(v_w - v')^{1/2} - \frac{1}{M}(u_w - u')^{1/2}\right] \tag{23a}$$

$$\overline{Z} = \left(\frac{2\omega}{a\beta\pi}\right)^{1/2}\left[(v_w - v')^{1/2} + \frac{1}{M}(u_w - u')^{1/2}\right] \tag{23b}$$

so that

$$dZ = d\overline{Z} = -\frac{1}{2}\left(\frac{2\omega}{a\beta\pi}\right)^{1/2} \frac{dv'}{(v_w - v')^{1/2}}$$

Then equation (22a) can be written as:

$$\phi(u_w, v_w, +0, t) = \frac{U\bar{\alpha}e^{i\omega t}}{M\pi}\left(\frac{2\omega}{a\beta\pi}\right)^{-1/2} \int_{v_w/k_2}^{u_w} \frac{du' e^{-\frac{i\omega\beta}{aM^2}(u_w - u')}}{(u_w - u')^{1/2}} \left(\int_{Z_1}^{Z_2} dZ e^{-\frac{i\pi}{2}Z^2} + \int_{\bar{Z}_1}^{\bar{Z}_2} d\bar{Z} e^{-\frac{i\pi}{2}\bar{Z}^2} \right)$$

$$= \frac{U\bar{\alpha}e^{i\omega t}}{M\pi}\left(\frac{2\omega}{a\beta\pi}\right)^{-1/2} \int_{v_w/k_2}^{u_w} \frac{du' e^{-\frac{i\omega\beta}{aM^2}(u_w - u')}}{(u_w - u')^{1/2}} \left\{ -C(Z_1) - C(\bar{Z}_1) + i\left[S(Z_1) + S(\bar{Z}_1) \right] \right\} \quad (24)$$

where

$$Z_1 = \left(\frac{2\omega}{a\beta\pi}\right)^{1/2} \left[(v_w - k_1 u')^{1/2} - \frac{1}{M}(u_w - u')^{1/2} \right] \quad \text{corresponding to} \quad v' = k_1 u' \quad (25a)$$

$$Z_2 = -\frac{1}{M}\left(\frac{2\omega}{a\beta\pi}\right)^{1/2} (u_w - u')^{1/2} \quad \text{corresponding to} \quad v' = v_w \quad (25b)$$

$$\bar{Z}_1 = \left(\frac{2\omega}{a\beta\pi}\right)^{1/2} \left[(v_w - k_1 u')^{1/2} + \frac{1}{M}(u_w - u')^{1/2} \right] \quad \text{corresponding to} \quad v' = k_1 u' \quad (25c)$$

$$\bar{Z}_2 = \frac{1}{M}\left(\frac{2\omega}{a\beta\pi}\right)^{1/2} (u_w - u')^{1/2} \quad \text{corresponding to} \quad v' = v_w \quad (25d)$$

Now introduce another new variable Y instead of u':

$$Y = \left(\frac{2\omega\beta}{\pi a M^2}\right)^{1/2}(u_w - u')^{1/2} \tag{26}$$

so that

$$dY = -\frac{1}{2}\left(\frac{2\omega\beta}{\pi a M^2}\right)^{1/2}\frac{du'}{(u_w - u')^{1/2}}$$

$$Z_1 = \left[\frac{2\omega}{a\beta\pi}(v_w - k_1 u_w) + \frac{k_1 M^2}{\beta^2}Y^2\right]^{1/2} - \frac{Y}{\beta} \tag{27a}$$

$$Z_2 = -\frac{Y}{\beta} \tag{27b}$$

$$\overline{Z}_1 = \left[\frac{2\omega}{a\beta\pi}(v_w - k_1 u_w) + \frac{k_1 M^2}{\beta^2}Y^2\right]^{1/2} + \frac{Y}{\beta} \tag{27c}$$

$$\overline{Z}_2 = \frac{Y}{\beta} = -Z_2 \tag{27d}$$

If

$$Y_1 = \left(\frac{2\omega\beta}{\pi a M^2}\right)^{1/2}\left(u_w - \frac{v_w}{k_2}\right)^{1/2}$$

then equation (24) becomes:

$$\phi(u_w, v_w, +0, t) = \frac{U\tilde{a}a}{\omega} e^{i\omega t} \int_0^{Y_1} dY e^{-\frac{i\pi}{2}Y^2} \begin{bmatrix} -C(Z_1) + iS(Z_1) \\ -C(\bar{Z}_1) + iS(\bar{Z}_1) \end{bmatrix} \tag{28}$$

At this stage more Fresnal integrals can be introduced by integrating by parts. For this purpose, the following properties of a Fresnal integral may be useful:

$$C(\epsilon) - iS(\epsilon) = \int_0^{\epsilon} e^{-\frac{i\pi}{2}(\epsilon')^2} d\epsilon' = \frac{1}{2}\int_0^{\frac{\pi\epsilon^2}{2}} \left[J_{-1/2}(\alpha') - iJ_{1/2}(\alpha')\right] d\alpha'$$

$$= \frac{1}{2}\int_0^{\frac{\pi\epsilon^2}{2}} H_{-1/2}^{(2)}(\alpha')\, d\alpha' \tag{29a}$$

$$\left(\alpha' = \frac{\pi}{2}\epsilon^2\right)$$

$$\int_0^{\epsilon} S(\epsilon')\, d\epsilon' = \epsilon S(\epsilon) + \frac{1}{\pi}\cos\frac{\pi}{2}\epsilon^2 - \frac{1}{\pi} \tag{29b}$$

$$\int_0^{\epsilon} C(\epsilon')\, d\epsilon' = \epsilon C(\epsilon) - \frac{1}{\pi}\sin\frac{\pi}{2}\epsilon^2 \tag{29c}$$

$$C(\epsilon) = J_{\frac{1}{2}}\left(\frac{\pi}{2}\epsilon^2\right) + J_{\frac{5}{2}}\left(\frac{\pi}{2}\epsilon^2\right) + J_{\frac{9}{2}}\left(\frac{\pi}{2}\epsilon^2\right) + \cdots = \sum_{n=0}^{\infty} J_{\frac{1}{2}+2n}\left(\frac{\pi}{2}\epsilon^2\right) \tag{29d}$$

$$S(\epsilon) = J_{\frac{3}{2}}\left(\frac{\pi}{2}\epsilon^2\right) + J_{\frac{7}{2}}\left(\frac{\pi}{2}\epsilon^2\right) + J_{\frac{11}{2}}\left(\frac{\pi}{2}\epsilon^2\right) + \cdots = \sum_{n=0}^{\infty} J_{\frac{3}{2}+2n}\left(\frac{\pi}{2}\epsilon^2\right) \tag{29e}$$

where $J(\ )$ is the Bessel function and $H^{(2)}(\ )$ is the Hankel function of the second kind and various subscripts indicate the order of these functions. For large values of ϵ,

$$C(\epsilon) = \frac{1}{2} + \frac{1}{\pi\epsilon} \sin \frac{\pi}{2}\epsilon^2 + O\left(\frac{1}{\epsilon^2}\right) \tag{29f}$$

$$S(\epsilon) = \frac{1}{2} - \frac{1}{\pi\epsilon} \cos \frac{\pi}{2}\epsilon^2 + O\left(\frac{1}{\epsilon^2}\right) \tag{29g}$$

$$S(\pm\infty) = C(\pm\infty) = \pm\infty \tag{29h}$$

$$S(\epsilon) = -S(-\epsilon), \quad C(\epsilon) = -C(-\epsilon) \tag{29i}$$

For details, see reference 10, pages 544 to 546 and 744 to 745, and also reference 11.

However, it is difficult, if not impossible, to reduce equation (28) to a closed form. Besides, there is usually more interest in the pressure coefficient which is generally known as:

$$C_p(x,y,t) = -\frac{2}{U^2}\frac{\partial \phi}{\partial t} - \frac{2}{U}\frac{\partial \phi}{\partial x} \tag{30}$$

rather than the potential itself. In the u,v coordinate system, the pressure coefficient is given by:

$$C_p(x,y,+0,t) = -\frac{2}{U^2}\frac{\partial \phi}{\partial t} - \frac{2}{U}\left(\frac{\partial \phi}{\partial u_w}\frac{\partial u_w}{\partial x} + \frac{\partial \phi}{\partial v_w}\frac{\partial v_w}{\partial x}\right)$$

$$= -\frac{2}{U^2}\frac{\partial \phi}{\partial t} - \frac{M}{U\beta}\left(\frac{\partial \phi}{\partial u_w} + \frac{\partial \phi}{\partial v_w}\right) \tag{31}$$

Now,

$$\frac{\partial \phi}{\partial t} = i\omega\phi(u_w, v_w, +0, t) \tag{32}$$

Differentiating equation (28) with respect to u_w and v_w,

$$\frac{\partial \phi}{\partial u_w} = \frac{U\beta\bar{a}e^{i\omega t}}{\pi M^2} \frac{e^{-\frac{i\pi}{2} Y_1^2}}{Y_1} \left\{ -C(Z_3) - C(\bar{Z}_3) + i\left[S(Z_3) + S(\bar{Z}_3)\right] \right\} +$$

$$\frac{Uk_1\bar{a}e^{i\omega t}}{\pi} \int_0^{Y_1} e^{-\frac{i\pi}{2} Y^2} dY \left(\frac{e^{-\frac{i\pi}{2} Z_1^2}}{\beta Z_1 + Y} + \frac{e^{-\frac{i\pi}{2} \bar{Z}_1^2}}{\beta \bar{Z}_1 - Y} \right) \tag{33}$$

$$\frac{\partial \phi}{\partial v_w} = -\frac{1}{k_2} \frac{U\beta\bar{a}e^{i\omega t}}{\pi M^2} \frac{e^{-\frac{i\pi}{2} Y_1^2}}{Y_1} \left[C(Z_3) - C(\bar{Z}_3) + iS(Z_3) + iS(\bar{Z}_3) \right] -$$

$$\frac{U\bar{a}e^{i\omega t}}{\pi} \int_0^{Y_1} e^{-\frac{i\pi}{2} Y^2} dY \left(\frac{e^{-\frac{i\pi}{2} Z_1^2}}{\beta Z_1 + Y} + \frac{e^{-\frac{i\pi}{2} \bar{Z}_1^2}}{\beta \bar{Z}_1 - Y} \right) \tag{34}$$

where

$$Z_3 = \left[\frac{2\omega}{a\beta\pi} (v_w - k_1 u_w) + \frac{k_1 M^2}{\beta^2} Y_1^2 \right]^{1/2} - \frac{Y_1}{\beta} \tag{35a}$$

$$\bar{Z}_3 = \left[\frac{2\omega}{a\beta\pi} (v_w - k_1 u_w) + \frac{k_1 M^2}{\beta^2} Y_1^2 \right]^{1/2} + \frac{Y_1}{\beta} \tag{35b}$$

The pressure coefficient is then given by:

$$C_p(x,y,+0,t) = \bar{\alpha}e^{i\omega t}\left(\frac{1}{M\pi}\left(\frac{1-k_2}{k_2}\right)\frac{1}{Y_1}\,e^{-\frac{i\pi}{2}Y_1^2}\left[-C(Z_3) - C(\bar{Z}_3) + iS(Z_3) + iS(\bar{Z}_3)\right] + \int_0^{Y_1} dY\, e^{-\frac{i\pi}{2}Y^2}\left\{-\frac{2i}{M}\left[-C(Z_1) - C(\bar{Z}_1) + iS(Z_1) + iS(\bar{Z}_1)\right] + \frac{M}{\pi\beta}(1-k_1)\left(\frac{e^{-\frac{i\pi}{2}Z_1^2}}{\beta Z_1 + Y} + \frac{e^{-\frac{i\pi}{2}\bar{Z}_1^2}}{\beta\bar{Z}_1 - Y}\right)\right\}\right) \qquad (36)$$

The above equation is used to calculate C_p along the trailing edge of a rectangular wing tip which is harmonically oscillating. (See fig. 5.) In this particular instance, $M = \sqrt{2}$, the frequency parameter $\frac{\omega c}{a\beta^2} = 0.2$, and the chord c is taken as unity. The curve is plotted in the form $\frac{C_p}{\bar{\alpha}e^{i\omega t}}$ against y (positive y measured outward along the span) so that for any specified amplitude of oscillation $\bar{\alpha}$ the pressure distribution at any instant t can be estimated from a single curve. As $\frac{C_p}{\bar{\alpha}e^{i\omega t}}$ is a complex quantity, the real and imaginary parts, denoted by $\left(\frac{C_p}{\bar{\alpha}e^{i\omega t}}\right)_R$ and $\left(\frac{C_p}{\bar{\alpha}e^{i\omega t}}\right)_I$, respectively, are plotted separately. If the harmonic oscillation is $\bar{\alpha}\cos\omega t$, that is, the real part of $\bar{\alpha}e^{i\omega t}$, then C_p can be calculated from:

$$C_p\left(\frac{x}{c},\frac{y}{c},t\right) = \bar{\alpha}\left[\left(\frac{C_p}{\bar{\alpha}e^{i\omega t}}\right)_R \cos\omega t - \left(\frac{C_p}{\bar{\alpha}e^{i\omega t}}\right)_I \sin\omega t\right] \qquad (37a)$$

Similarly, if the oscillation is $\bar{\alpha} \sin \omega t$, that is, the imaginary part of $\bar{\alpha} e^{i\omega t}$, it is given by:

$$C_p\left(\frac{x}{c}, \frac{y}{c}, t\right) = \bar{\alpha}\left[\left(\frac{C_p}{\bar{\alpha} e^{i\omega t}}\right)_R \sin \omega t + \left(\frac{C_p}{\bar{\alpha} e^{i\omega t}}\right)_I \cos \omega t\right] \tag{37b}$$

It is interesting to note that when $y = 1$ these values conform with the two-dimensional values given in reference 6.

As soon as C_p everywhere over the wing tip is known, it is simple to obtain C_L, C_D, and C_M graphically.

As far as the calculation of the center section is concerned, it is easy to show that (see fig. 4)

$$\phi(u_w, v_w, +0, t) = -\frac{U\bar{\alpha}}{2M\pi} \int_0^{u_w} \frac{du'}{(u_w - u')^{1/2}} \int_{k_2' u'}^{v_w} \frac{dv'}{(v_w - v')^{1/2}} \left[e^{i\omega(t-\tau_1)} + e^{i\omega(t-\tau_2)}\right] -$$

$$\frac{U\bar{\alpha}}{2M\pi} \int_{v_w/k_1'}^{0} \frac{du'}{(u_w - u')^{1/2}} \int_{k_1' u'}^{v_w} \frac{dv'}{(v_w - v')^{1/2}} \left[e^{i\omega(t-\tau_1)} + e^{i\omega(t-\tau_2)}\right] \tag{38}$$

where

$$\tau_1 = \frac{1}{a\beta}\left[v_w - v' + u_w - u' - \frac{2}{M}(u_w - u')^{1/2}(v_w - v')^{1/2}\right]$$

$$\tau_2 = \frac{1}{a\beta}\left[v_w - v' + u_w - u' + \frac{2}{M}(u_w - u')^{1/2}(v_w - v')^{1/2}\right]$$

Introducing Z and $\bar{Z}$ as before (cf. equations (23)), and then following the procedure of deriving equation (24), equation (28) can be written as:

$$\phi(u,v,+0,t) = \frac{U\tilde{a}e^{i\omega t}}{\pi M}\left(\frac{2\omega}{a\beta\pi}\right)^{1/2}\int_0^{u_w}\frac{e^{\frac{-i\omega\beta}{aM^2}(u_w-u')}du'}{(u_w - u')^{1/2}}\left[-C(Z_1') - C(\bar{Z}_1') + iS(Z_1') + iS(\bar{Z}_1')\right] +$$

$$\frac{U\tilde{a}e^{i\omega t}}{\pi M}\left(\frac{2\omega}{a\beta\pi}\right)^{1/2}\int_{v_w/k_1}^{0}\frac{e^{\frac{-i\omega\beta}{aM^2}(u_w-u')}du'}{(u_w - u')^{1/2}}\left[-C(Z_1'') - C(\bar{Z}_1'') + iS(Z_1'') + iS(\bar{Z}_1'')\right] \quad (39)$$

where, replacing k_1 by k_2',

$Z_1' = Z_1$ in equation (25a)

$\bar{Z}_1' = \bar{Z}_1$ in equation (25c)

and, replacing k_1 by k_1',

$$Z_1'' = Z_1 \quad \text{in equation (25a)}$$

$$\bar{Z}_1'' = \bar{Z}_1 \quad \text{in equation (25c)}$$

Similarly Y can be defined as in equation (26) and by the same procedure C_p can be determined.

APPROXIMATE ANALYTIC SOLUTIONS OF PRESSURE ON AN OSCILLATING FINITE WING - SECOND METHOD

In the preceding section, an approximate integral solution for the oscillating finite wing is given, and an example of calculation is shown, but the full evaluation of the integral for a large number of cases would take more time than was available. However, for very low frequencies, this problem can be solved asymptotically by using a few terms of a series expansion of $w(u,v,t)$. In the following section the approximate analytic expressions will be shown.

Analysis

From equation (22a),

$$\phi_T(x,y,+0,t) = -\frac{U\bar{\alpha}e^{i\omega t}}{2\pi\beta^2}\iint_{S_{w1}} \frac{e^{i\omega\tau_1} + e^{i\omega\tau_2}}{r}\, d\xi\, d\eta \qquad (40)$$

where S_{w1} is the area PABC as shown in figure 6. Since the two-dimensional solution with supersonic leading edge is known, the potential can be obtained alternatively by calculating the contribution of S_{wa}

which is the area BCD, the difference between the two-dimensional source area PAD and S_{w1} as shown in figure 6. Then,

$$\phi_T(x,y,+0,t) = -\frac{U\bar{\alpha}e^{i\omega t}}{2\pi\beta^2}\left(\iint_{S_{w1}+S_{wa}} \frac{e^{-i\omega\tau_1} + e^{-i\omega\tau_2}}{r}\, d\xi\, d\eta - \iint_{S_{wa}} \frac{e^{-i\omega\tau_1} + e^{-i\omega\tau_2}}{r}\, d\xi\, d\eta\right)$$

$$= \phi_o(x,y,+0,t) - \overline{\phi}(x,y,+0,t) \tag{41}$$

$$\overline{\phi}(x,y,+0,t) = -\frac{U\bar{\alpha}e^{i\omega t}}{2\pi\beta^2}\iint_{S_{wa}} \frac{e^{-i\omega\tau_1} + e^{-i\omega\tau_2}}{r}\, d\xi\, d\eta$$

$$= -\frac{1}{\pi\beta^2}\iint_{S_{wa}} \frac{w(\xi,\eta,+0,t-\tau_1) + w(\xi,\eta,+0,t-\tau_2)}{r}\, d\xi\, d\eta \tag{42}$$

The variables τ_1, τ_2, r, and w are the same as before. In this development, it is found more convenient to introduce a new coordinate system as follows: The x'-axis passing through the fixed point (x,y) runs upward along the right forward Mach line. The origin is taken as the point where the x'-axis intersects the wing-tip side edge. The y'-axis following the other Mach line runs left upward as shown in figure 6. The origin of the x',y' coordinate system is translated from the origin of the x,y system a distance $\frac{\beta\delta}{M}$, where δ can be shown to be

$$\delta = \frac{M}{\beta}(x + \beta y) \tag{43}$$

which is a function of the point $P(x,y)$ only. The transformation relations are

$$\left.\begin{aligned}
x' &= -\frac{M}{2\beta}\left(x - \frac{\beta}{M}\delta - \beta y\right) = -\frac{1}{2}\left(\frac{M}{\beta}x - My - \delta\right) & x &= -\frac{\beta}{M}(x' + y' - \delta) \\
y' &= -\frac{M}{2\beta}\left(x - \frac{\beta}{M}\delta + \beta y\right) = -\frac{1}{2}\left(\frac{M}{\beta}x + My - \delta\right) & y &= \frac{1}{M}(x' - y') \\
\xi' &= -\frac{M}{2\beta}\left(\xi - \frac{\beta}{M}\delta - \beta\eta\right) & \xi &= -\frac{\beta}{M}(\xi' + \eta' - \delta) \\
\eta' &= -\frac{M}{2\beta}\left(\xi - \frac{\beta}{M}\delta + \beta\eta\right) & \eta &= \frac{1}{M}(\xi' - \eta') \\
\frac{\partial(x',y')}{\partial(x,y)} &= \frac{M^2}{2\beta}
\end{aligned}\right\} \tag{44}$$

and

$$\left.\begin{aligned}
r &= \frac{2}{\beta M}\sqrt{(-\eta')(x' - \xi')} = \frac{2}{\beta M}\sqrt{\eta'(\xi' - x')} \\
\tau_1 &= \frac{1}{a\beta}\left[(\xi' + \eta' - x') - \frac{2}{M}\sqrt{\eta'(\xi' - x')}\right] \\
\tau_2 &= \frac{1}{a\beta}\left[(\xi' + \eta' - x') + \frac{2}{M}\sqrt{\eta'(\xi' - x')}\right]
\end{aligned}\right\} \tag{45}$$

Now $e^{-i\omega\tau_1}$ and $e^{-i\omega\tau_2}$ can be expanded in terms of the new variables

$$e^{-i\omega\tau_1} = \sum_{n=0}^{\infty} \frac{(-i\omega\tau_1)^n}{n!} = \sum_{n=0}^{\infty} (-i)^n \frac{\omega^n}{n!} \tau_1^n$$

$$= \sum_{n=0}^{\infty} \frac{(-i)^n}{n!} \left(\frac{\omega}{a\beta}\right)^n \left(\mu + \eta' - \frac{2}{M}\sqrt{\eta'\mu}\right)^n \tag{46}$$

where $\mu = \xi' - x'$ is introduced.

Similarly,

$$e^{-i\omega\tau_2} = \sum_{n=0}^{\infty} \frac{(-i)^n}{n!} \left(\frac{\omega}{a\beta}\right)^n \left(\mu + \eta' + \frac{2}{M}\sqrt{\eta'\mu}\right)^n \tag{47}$$

If attention is restricted to $|\omega\tau_1| < 1$ and $|\omega\tau_2| < 1$, $e^{-i\omega\tau_1}$ and $e^{-i\omega\tau_2}$ can be approximately represented by a few terms of the series. In the later development, five terms of each series are used. Of course, for higher values of $|\omega\tau_1|$ and $|\omega\tau_2|$ more terms should be used. Introducing this approximation into equation (42),

$$\bar{\phi}(x',y',+0,t) = -\frac{U\bar{\alpha}e^{i\omega t}}{\pi\beta M^2} \int_{-x'}^{\frac{\beta\delta}{\beta+k}-x'} d\mu \int_{\frac{\beta+k}{\beta-k}(\mu+x')}^{\frac{\beta\delta}{\beta-k}} \frac{d\eta'}{r}\left(e^{-i\omega\tau_1} + e^{-i\omega\tau_2}\right)$$

$$= -\frac{U\bar{\alpha}e^{i\omega t}}{2\pi M} \int_{-x'}^{\frac{\beta\delta}{\beta+k}-x'} d\mu \int_{0}^{\frac{\beta\delta}{\beta-k}-\frac{\beta+k}{\beta-k}(\mu+x')} \frac{d\eta'}{(\eta'\mu)^{1/2}} \left[2 - \frac{2i\omega}{a\beta}(\mu+\eta') - \frac{\omega^2}{a^2\beta^2}(\mu+\eta')^2 + \frac{i\omega^3}{a^3\beta^3}(\mu+\eta')^3 + \right.$$

$$\left. \frac{\omega^4}{12a^4\beta^4}(\mu+\eta')^4 + 4\eta'\mu\left[-\frac{\omega^2}{a^2M^2\beta^2} + \frac{i\omega^3}{a^3M^3\beta^3}(\mu+\eta') + \frac{\omega^4}{2a^4M^2\beta^4}(\mu+\eta')^2\right] + \frac{4}{3}\frac{\omega^4}{a^4M^4\beta^4}(\eta')^2\mu^2\right] \tag{48}$$

Integrating with respect to η' and introducing a group of new notations,

$$\bar{\phi}(x',y',+0,t) = \frac{-\sqrt{2\gamma_2}U\bar{\alpha}e^{i\omega t}}{\pi M\sqrt{\gamma_1}} \int_0^{\frac{\beta\delta}{\beta-k}} dz \left[\frac{1}{\sqrt{b - z^2}} \left(e_2 z^2 + e_4 z^4 + e_6 z^6 + e_8 z^8 + e_{10} z^{10} \right) + \sqrt{b - z^2} \left(g_4 z^4 + g_6 z^6 + g_8 z^8 \right) + \left(b - z^2 \right)^{3/2} h_6 z^6 \right] \tag{49}$$

where $\gamma_1 = \frac{1}{\beta - k}$, $\gamma_2 = \frac{1}{\beta + k}$, $z^2 = b - \frac{\gamma_1}{\gamma_2}\mu$, $b = \beta\gamma_1\delta - \frac{\gamma_1}{\gamma_2}x'$, and the e's, g's, and h_6 are given in appendix B. With the aid of the formulas in appendix C, the following integration of equation (49) can be carried out with respect to z:

$$\begin{aligned}\bar{\phi}(x,y,+0,t) = -\frac{U}{2\pi}\bar{\alpha}e^{i\omega t}\Bigg[& \sin^{-1}\sqrt{\frac{x + \beta y}{x - ky}} \sum_{n=1}^{5} \sigma_{1,n}(x - ky)^n + \sqrt{-y(x + \beta y)} \sum_{n=0}^{4} \sigma_{2,n}(x - ky)^n + \\ & \sqrt{-y(x + \beta y)^3} \sum_{n=0}^{3} \sigma_{3,n}(x - ky)^n + \sqrt{-y(x + \beta y)^5} \sum_{n=0}^{2} \sigma_{4,n}(x - ky)^n + \\ & \sqrt{-y(x + \beta y)^7} \sum_{n=0}^{1} \sigma_{5,n}(x - ky)^n + \sqrt{-y(x + \beta y)^9}\, \sigma_{6,0} + \\ & \sqrt{-y^3(x + \beta y)} \sum_{n=1}^{3} \sigma_{7,n}(x - ky)^n + \sqrt{-y^3(x + \beta y)^3} \sum_{n=0}^{2} \sigma_{8,n}(x - ky)^n + \\ & \sqrt{-y^3(x + \beta y)^5} \sum_{n=0}^{1} \sigma_{9,n}(x - ky)^n + \sqrt{-y^3(x + \beta y)^7}\, \sigma_{10,0} \Bigg]\end{aligned} \tag{50}$$

where the $\sigma_{m,n}$'s (m and n are integers) in terms of $\bar{\omega}$, k, M, and β are given in appendix B. By definition,

$$\bar{C}_p = -\frac{2}{U^2}\frac{\partial\bar{\phi}}{\partial t} - \frac{2}{U}\frac{\partial\bar{\phi}}{\partial x} \tag{51}$$

Differentiating equation (50) with respect to t,

$$-\frac{2}{U^2}\frac{\partial\bar{\phi}}{\partial t} = -\frac{2i\omega}{U^2}\bar{\phi} \tag{52}$$

Differentiating equation (50) with respect to x and adding equation (52),

$$\bar{C}_p(x,y,+0,t) = \frac{1}{\pi}\bar{\alpha}e^{i\omega t}\left\{\sin^{-1}\sqrt{\frac{x+\beta y}{x-ky}}\left[\sum_{n=1}^{5} n\sigma_{1,n}(x-ky)^{n-1} + \frac{i\omega}{U}\sum_{n=1}^{5}\sigma_{1,n}(x-ky)^n\right] + \right.$$

$$\sqrt{-y(x+\beta y)}\left[\sum_{n=1}^{4} n\sigma_{2,n}(x-ky)^{n-1} + \frac{i\omega}{U}\sum_{n=0}^{4}\sigma_{2,n}(x-ky)^n + \frac{3}{2}\sum_{n=0}^{3}\sigma_{3,n}(x-ky)^n + \right.$$

$$\left.\sum_{n=1}^{3}\overline{\sigma_{2,n}}(x-ky)^n\right] + \sqrt{-y(x+\beta y)^3}\left[\sum_{n=1}^{3} n\sigma_{3,n}(x-ky)^{n-1} + \frac{i\omega}{U}\sum_{n=0}^{3}\sigma_{3,n}(x-ky)^n + \right.$$

$$\left.\frac{5}{2}\sum_{n=0}^{2}\sigma_{4,n}(x-ky)^n\right] + \sqrt{-y(x+\beta y)^5}\left[\sum_{n=1}^{2} n\sigma_{4,n}(x-ky)^{n-1} + \frac{i\omega}{U}\sum_{n=0}^{2}\sigma_{4,n}(x-ky)^n + \right.$$

$$\left.\frac{7}{2}\sum_{n=0}^{1}\sigma_{5,n}(x-ky)^n\right] + \sqrt{-y(x+\beta y)^7}\left[\sigma_{5,1} + \frac{i\omega}{U}\sum_{n=0}^{1}\sigma_{5,n}(x-ky)^n + \frac{9}{2}\sigma_{6,0}\right] +$$

$$\sqrt{-y(x+\beta y)^9}\left(\frac{i\omega}{U}\sigma_{6,0}\right) + \sqrt{-y^3(x+\beta y)}\left[\sum_{n=1}^{3} n\sigma_{7,n}(x-ky)^{n-1} + \frac{i\omega}{U}\sum_{n=1}^{3}\sigma_{7,n}(x-ky)^n + \right.$$

$$\left.\frac{3}{2}\sum_{n=0}^{2}\sigma_{8,n}(x-ky)^n\right] + \sqrt{-y^3(x+\beta y)^3}\left[\sum_{n=1}^{2} n\sigma_{8,n}(x-ky)^{n-1} + \frac{i\omega}{U}\sum_{n=0}^{2}\sigma_{8,n}(x-ky)^n + \right.$$

$$\left.\frac{5}{2}\sum_{n=0}^{1}\sigma_{9,n}(x-ky)^n\right] + \sqrt{-y^3(x+\beta y)^5}\left[\sigma_{9,1} + \frac{i\omega}{U}\sum_{n=0}^{1}\sigma_{9,n}(x-ky)^n + \frac{7}{2}\sigma_{10,0}\right] +$$

$$\left.\sqrt{-y(x+\beta y)^7}\,\frac{i\omega}{U}\,\sigma_{10,0}\right\} \qquad (53)$$

where again the $\sigma_{m,n}$'s are given in appendix B. The actual pressure coefficient is

$$C_p = -\frac{2}{U^2}\frac{\partial \phi_T}{\partial t} - \frac{2}{U}\frac{\partial \phi_T}{\partial x}$$

$$= -\frac{2}{U^2}\frac{\partial \phi_o}{\partial t} - \frac{2}{U}\frac{\partial \phi_o}{\partial x} - \left(-\frac{2}{U^2}\frac{\partial \bar{\phi}}{\partial t} - \frac{2}{U}\frac{\partial \bar{\phi}}{\partial x}\right)$$

$$= C_{po}(x,y,0,t) - \bar{C}_p(x,y,0,t) \qquad (54)$$

where $\phi_T = \phi_o - \bar{\phi}$ as given in equation (41) and $C_{po}(x,y,0,t)$ is the pressure coefficient of the two-dimensional case as given in reference 5.

Rectangular Wing Tip

For the rectangular wing ($k = 0$) equations (53) and (54) reduce to

$$C_p(x,y,+0,t) = \frac{1}{\pi}\bar{\alpha}e^{i\omega t}\left[\sin^{-1}\sqrt{\frac{x+\beta y}{x}}\sum_{n=0}^{5} a_n x^n + \sqrt{-y(x+\beta y)}\sum_{n=0}^{4} b_n x^n + \right.$$

$$\sqrt{-y(x+\beta y)^3}\sum_{n=0}^{3} c_n x^n + \sqrt{-y(x+\beta y)^5}\sum_{n=0}^{2} d_n x^n +$$

$$\sqrt{-y(x+\beta y)^7}\sum_{n=0}^{1} e_n x^n + \sqrt{-y(x+\beta y)^9}\, f +$$

$$\sqrt{-y^3(x+\beta y)}\sum_{n=0}^{3} g_n x^n + \sqrt{-y^3(x+\beta y)^3}\sum_{n=0}^{2} h_n x^n +$$

$$\left.\sqrt{-y^3(x+\beta y)^5}\sum_{n=0}^{1} i_n x^n + \sqrt{-y^3(x+\beta y)^7}\, j\right] \qquad (55)$$

where the a's, b's, c's, d's, e's, f, g's, h's, i's, and j are given in appendix B. (The particular $\sigma_{m,n}$'s for $k = 0$ are found in appendix B.)

Average Pressure Coefficient over Rectangular Wing Tip

For engineering purposes, an average value of $C_{p,av}$ over the entire tip influenced by the three-dimensional flow may be useful. (Assume unit tip chord.)

$$C_{p,av} = \frac{1}{2\beta}\int_0^1 dx \int_0^{-x/\beta} dy C_p$$

$$= \frac{-1}{2\beta}\int_0^1 dx \int_0^{-x/\beta} dy\left[\bar{C}_p(x,y) - \bar{C}_p(x + \beta y, +0)\right]$$

$$= C_{p1} + C_{p2} \tag{56}$$

where 2β is the wing-tip area influenced by three-dimensional flow.

$$C_{p1} = \frac{-1}{2\pi\beta}\bar{\alpha}e^{i\omega t}\int_0^1 dx \sum_{n=0}^{5} a_n x^n \int_0^{-x/\beta} dy\left(\sin^{-1}\sqrt{\frac{x + \beta y}{x}} - \frac{\pi}{2}\right)$$

$$= \frac{-1}{4\beta\pi}\bar{\alpha}e^{i\omega t}\int_0^1 dx \sum_{n=0}^{5} a_n x^n \int_{-1}^{1} \cos^{-1} q \, dq$$

$$= \frac{-1}{4\beta}\bar{\alpha}e^{i\omega t}\sum_{n=0}^{5}\frac{a_n}{n+2} \tag{57}$$

where

$$\frac{x + 2\beta y}{x} = q$$

$$C_{p2} = \frac{-1}{2\beta\pi}\bar{\alpha}e^{i\omega t}\int_0^1 dx \int_0^{-x/\beta} dy\left[\sqrt{-y(x+\beta y)}\sum_{n=0}^{4} b_n x^n + \sqrt{-y(x+\beta y)^3}\sum_{n=0}^{3} c_n x^n + \sqrt{-y(x+\beta y)^5}\sum_{n=0}^{2} d_n x^n + \sqrt{-y(x+\beta y)^7}\sum_{n=0}^{1} e_n x^n + \sqrt{-y(x+\beta y)^9}\, f + \sqrt{-y^3(x+\beta y)}\sum_{n=0}^{3} g_n x^n + \sqrt{-y^3(x+\beta y)^3}\sum_{n=0}^{2} h_n x^n + \sqrt{-y^3(x+\beta y)^5}\sum_{n=0}^{1} i_n x^n + \sqrt{-y^3(x+\beta y)^7}\, j\right] \tag{58a}$$

Let $\beta y = -z^2$. Expanding higher powers in terms of $(x - z^2)^{1/2}x^k z^{2s}$, the integral may be integrated by formula (C2) in appendix C to

$$C_{p2} = \frac{-1}{4\beta}\bar{\alpha}e^{i\omega t}\int_0^1 dx\left(b_1'x^2 + b_2'x^3 + b_3'x^4 + b_4'x^5 + b_5'x^6\right)$$

$$= \frac{-1}{4\beta}\bar{\alpha}e^{i\omega t}\sum_{n=1}^{5}\frac{b_n'}{n+2} \tag{58b}$$

The b_n''s are given in appendix B. Hence,

$$C_{p,av} = \frac{-1}{4\beta}\bar{\alpha}e^{i\omega t}\sum_{n=0}^{5}\frac{a_n + b_n'}{n+2} = -\bar{\alpha}e^{i\omega t}\sum_{n=0}^{5} c_n' \tag{59}$$

(See appendix B.)

Calculations and Graphs

Owing to the complicated nature of the formulas in this section, the calculations are rather tedious. The calculations are too long to be included here, but the essential results are summarized in figures 7

to 15. The pressure coefficient given in this paper is referred to a point on the upper surface of the wing. Figures 7 to 10 give the pressure distribution on a rectangular wing tip of unit chord with different free-stream flight Mach numbers. The frequency parameter $\frac{\omega c}{a}$ is taken as 0.2 in these calculations. As before the complex quantity $\frac{\pi C_p}{\bar{\alpha} e^{i\omega t}}$ is used and plotted in two parts - real and imaginary (e.g., figs. 7(a) and 7(b)). These curves are plotted along the spanwise direction (y being negative when measured inward from the tip) at various percentages of chord. If $\frac{\pi C_p}{\bar{\alpha} e^{i\omega t}}$ along the chordwise direction is desired, some cross-plotting is necessary. It should be noted that these curves do not give the pressure coefficient C_p directly, but C_p may be calculated easily from them by using equation (37a) or (37b) or both.

Figure 7 is calculated for a Mach number of $\sqrt{2}$. (Note that figure 7 checks well with figure 5 which was calculated by the first method.) It is seen that $\left(\frac{\pi C_p}{\bar{\alpha} e^{i\omega t}}\right)_R$ is zero at the wing tip (see fig. 7(a)) for all values of x, except at the leading edge where $\left(\frac{\pi C_p}{\bar{\alpha} e^{i\omega t}}\right)_R$ becomes 2π, which is in agreement with the two-dimensional result along the Mach line $-y = x$. Taking the trailing edge ($x = 1.0$) as another example, $\left(\frac{\pi C_p}{\bar{\alpha} e^{i\omega t}}\right)_R$ increases from zero at the tip ($y = 0$) to a value of -1.885π at $-y = x = 1$. Thus it is seen that for this case $\left(\frac{\pi C_p}{\bar{\alpha} e^{i\omega t}}\right)_R$ varies very little along the left Mach line of the tip as is shown by the dotted line in figure 7(a). The horizontal solid line for $-y > 1.0$ is the two-dimensional result. The imaginary part $\left(\frac{\pi C_p}{\bar{\alpha} e^{i\omega t}}\right)_I$ shown in figure 7(b) is of a similar nature. Figures 8, 9, and 10 show the same wing oscillating under the same conditions except that the free-stream Mach number is now 2, 3, and 4, respectively. A few points may be of interest. As the Mach number increases, the maximum magnitudes of both $\left(\frac{\pi C_p}{\bar{\alpha} e^{i\omega t}}\right)_R$ and $\left(\frac{\pi C_p}{\bar{\alpha} e^{i\omega t}}\right)_I$ decrease, while the two-dimensional values become more nearly constant.

In order to show the accuracy of this method, a comparison between the result of the present approximate method and the two-dimensional values along the left Mach line of the tip cone is given in figure 11. The case considered is a rectangular wing tip ($k = 0$) and the free-stream Mach number is taken as $\sqrt{2}$. The solid line shown is the approximation and the dotted line is the exact one. At $\frac{\omega c}{a\beta^2} = 0.283$, the deviation is unnoticeable. At $\frac{\omega c}{a\beta^2} = 0.707$, which is beyond the imposed limit, the maximum deviation of the imaginary part amounts to 10 percent. The same curve at $x = 0.8$ corresponds to the case of $x/c = 1$ with lower frequency parameter $\frac{\omega c}{a\beta^2} = 0.707$; at $\frac{x}{c} = 0.5656$ the maximum deviation is of the order of 2 percent. Thus beyond $\frac{\omega c}{a\beta^2} = 0.5$ the approximation of the imaginary part is not very favorable unless more terms of the series expansion are taken.

There is another parameter which influences the accuracy of the present method, that is, the sweepback angle ($\Lambda = \tan^{-1} k$) of the supersonic leading edge. Figure 12 offers such a comparison. Here the Mach number is $\sqrt{2}$, $\frac{\omega c}{a\beta^2} = 0.283$, and the parameter k varies. The heavier line gives the two-dimensional exact results along the left tip Mach line, and the lighter line of the same kind gives $\frac{C_p}{\bar{\alpha}e^{i\omega t}}$ of the present method. Although $\frac{C_p}{\bar{\alpha}e^{i\omega t}}$ does show slight deviation from the exact value at higher values of k, the comparison is favorable.

In order to show some cases with high sweepback angle (although the leading edge is still supersonic), figure 13 gives the distribution of $\frac{C_p}{\bar{\alpha}e^{i\omega t}}$ over the three-dimensional wing tip of a 45° sweepback angle at $M = 2$. For a matter of convenience in calculation, the results are expressed in oblique coordinates $x + \beta y$ and $x - y$. The line $x + \beta y = \text{Constant}$ is parallel to the left Mach line, while $x - y = \text{Constant}$ is parallel to the leading edge. Here, the chord normal to the leading edge is chosen as unity. Therefore, $x - y$ represents percentage of chord. With such a definition of the chord, the chord c used in the frequency parameter $\frac{\omega c}{a\beta^2}$ should be considered as this normal chord. The circles at the left lower corner of figure 13(a) represent the values along the left Mach line. With the sketch on the figure, the general features of the curves are clear.

A comparison of results of this sweepback case with two-dimensional exact values of $\frac{C_p}{\bar{\alpha}e^{i\omega t}}$ is also shown in figure 14. The comparison is favorable. The two-dimensional value of $\frac{C_p}{\bar{\alpha}e^{i\omega t}}$ for a sweptback wing is obtained from reference 6.

For engineers, the pressure distribution on the three-dimensional wing tip is not of so much interest as the average pressure distribution $C_{p,av}$. Figure 15 calculated from equation (59) may serve such a purpose. The expression $C_L = -2C_{p,av}$ may be considered as the lift coefficient for the three-dimensional wing tip. The rectangular wing tip ($k = 0$) at various Mach numbers is considered. The dotted curves correspond to $\frac{\omega c}{a} = 0.2$, and the solid curves, to $\frac{\omega c}{a} = 0.5$. The magnitudes of both the real and the imaginary parts of $\frac{C_p}{\bar{\alpha}e^{i\omega t}}$ decrease with increasing Mach number as mentioned before. The change of $\frac{\omega c}{a}$ from 0.2 to 0.5 causes a slight drop in the real part of $\frac{C_p}{\bar{\alpha}e^{i\omega t}}$ but a greater drop in the imaginary part. The average pressure at $\frac{\omega c}{a} = 0.2$ deviates so little from the steady case ($\omega = 0$) that it is hard to show in figure 15(a).

The present method does give a closed expression, but it takes a great deal of time to calculate even a single point.

DISCUSSION OF RESULTS

With the above analysis, a few points should be emphasized. From Evvard's concept of the "diaphragm," the two approximate methods have been shown to give a satisfactory pressure distribution in the wing tip influenced by the three-dimensional flow, if the frequency parameter is low and if the leading and trailing edges are supersonic.

The comparison of the pressure coefficient obtained by the second method with two-dimensional exact solutions of linearized theory is favorable, if the frequency parameter $\frac{\omega c}{a\beta^2}$ is around 0.5 and the point is at the trailing edge. It is expected that the first method should

give satisfactory results with the frequency parameter of the order of one-half. Of course, if only the average pressure coefficient over the entire tip bounded by the left tip Mach line is wanted, a higher frequency parameter up to the order of unity may be used.

The effect of the three-dimensional flow on the wing tip is essentially to reduce the pressure increment in the area. With the approximation given by the present theory, the pressure coefficient at the tip side edge is zero except at the point on the leading edge. Of course, the exact theory would give finite values at the side edge, which would approach zero (as $\omega \longrightarrow 0$) as predicted by the conical-flow theory. At low values of the frequency parameter, the effects of the finite edge pressures give negligibly small contributions to the aerodynamic behavior of the wing as a whole. It is in this fact that the present methods find their justification.

The effect of increasing Mach number is to reduce the real and imaginary parts of $\frac{C_p}{\bar{\alpha}e^{i\omega t}}$ in magnitude, if the sweepback angle and the frequency parameter remain the same. If other conditions of the wing remain the same, increase of the sweepback angle causes the magnitude of the real part of $\frac{C_p}{\bar{\alpha}e^{i\omega t}}$ to increase and the imaginary part of it to decrease as shown in figure 12. Increase of frequency parameter has the opposite effect.

The pressure coefficient of a point influenced by the nose of the sweptback wing is given in terms of the Fresnal integral. It is not difficult to carry out the numerical integration for this case. In this portion of the wing, no approximation is used.

The first method of calculating C_p at the tip using the Fresnal integral appears worthy of more extensive study in the future as the method is very simple and useful. The second method gives closed expressions for C_p and $C_{p,av}$ and it has been investigated extensively in the present report.

The present analysis applies only to cases in which the flow at the leading and trailing edges is supersonic, and the nose Mach cone and the tip Mach cone do not intersect within the wing area. With slight modification the methods can be extended to more general wing plan forms.

The Johns Hopkins University
Baltimore, Md., November 15, 1949

APPENDIX A

SYMBOLS

a	velocity of sound
A	source strength
$b = \beta\gamma_1\delta - \frac{\gamma_1}{\gamma_2} x'$ (equation (49))	
c_n'	coefficients of $C_{p,av}$
c	chord
C_D	drag coefficient
C_L	lift coefficient
C_M	moment coefficient
C_p	pressure coefficient
$C(\epsilon)$	Fresnal integral $\left(\int_0^{\epsilon} \cos \frac{\pi}{2} (\epsilon')^2 \, d\epsilon'\right)$
$f(\ )$	function concerning source strength
$\dot{h}_{max}$	maximum descending rate
$\bar{i}$	unit vector in x-direction
k, k_1, k_1', k_2, k_2'	constants expressing wing inclination

M free-stream Mach number

$\bar{q}$ velocity vector

$\bar{q}'$ perturbation velocity vector

$$r = \frac{1}{M^2 - 1}\sqrt{(x - \xi)^2 - \left(M^2 - 1\right)\left[(y - \eta)^2 + (z - \zeta)^2\right]}$$

S surface

$S(\epsilon)$ Fresnal integral $\left(\int_0^{\epsilon} \sin \frac{\pi}{2}(\epsilon')^2 \, d\epsilon'\right)$ (see fig. 2)

t time

U free-stream velocity

u,v characteristic coordinates

u' source location along u-axis

v' source location along v-axis

w velocity component in z-direction

x longitudinal axis

x',y' transformed axes

y spanwise axis

$$Y = \left(\frac{2\omega\beta}{\pi a M^2}\right)^{1/2}\left(u_w - u'\right)^{1/2}$$

$$Y_1 = \left(\frac{2\omega\beta}{\pi a M^2}\right)^{1/2}\left(u_w - \frac{v_w}{k_2}\right)^{1/2}$$

z vertical axis

$$Z = \left(\frac{2\omega}{a\beta\pi}\right)^{1/2}\left[\left(v_w - v'\right)^{1/2} - \frac{1}{M}\left(u_w - u'\right)^{1/2}\right]$$

$$Z_1 = \left(\frac{2\omega}{a\beta\pi}\right)^{1/2}\left[\left(v_w - k_1u'\right)^{1/2} - \frac{1}{M}\left(u_w - u'\right)^{1/2}\right]$$

$$= \left[\frac{2\omega}{a\beta\pi}\left(v_w - k_1u_w\right) + \frac{k_1M^2}{\beta^2}Y^2\right]^{1/2} - \frac{Y}{\beta}$$

$$Z_2 = -\left(\frac{2\omega}{a\beta\pi}\right)^{1/2}\frac{1}{M}\left(u_w - u'\right)^{1/2} = -\frac{Y}{\beta}$$

$$Z_3 = \left[\frac{2\omega}{a\beta\pi}\left(v_w - k_1u_w\right) + \frac{k_1M^2}{\beta^2}Y_1^2\right]^{1/2} - \frac{Y_1}{\beta}$$

$$= \left(\frac{2\omega}{a\beta\pi}\right)^{1/2}\left[\left(v_w - \frac{k_1v_w}{k_2}\right)^{1/2} - \frac{1}{M}\left(u_w - \frac{v_w}{k_2}\right)^{1/2}\right]$$

$$\overline{Z} = \left(\frac{2\omega}{a\beta\pi}\right)^{1/2}\left[\left(v_w - v'\right)^{1/2} + \frac{1}{M}\left(u_w - u'\right)^{1/2}\right]$$

$$\overline{Z}_1 = \left(\frac{2\omega}{a\beta\pi}\right)^{1/2}\left[\left(v_w - k_1u'\right)^{1/2} + \frac{1}{M}\left(u_w - u'\right)^{1/2}\right]$$

$$= \left[\frac{2\omega}{a\beta\pi}\left(v_w - k_1u_w\right) + \frac{k_1M^2}{\beta^2}Y^2\right]^{1/2} + \frac{Y}{\beta}$$

$$\overline{Z}_2 = \left(\frac{2\omega}{a\beta\pi}\right)^{1/2}\frac{1}{M}\left(u_w - u\right)^{1/2} = \frac{Y}{\beta}$$

$$\bar{Z}_3 = \left[\frac{2\omega}{a\beta\pi}\left(v_w - k_1 u_w\right) + \frac{k_1 M^2}{\beta^2} Y_1^2\right]^{1/2} + \frac{Y_1}{\beta}$$

$$= \left(\frac{2\omega}{a\beta\pi}\right)^{1/2}\left[\left(v_w - \frac{k_1 v_w}{k_2}\right)^{1/2} + \frac{1}{M}\left(u_w - \frac{v_w}{k_2}\right)^{1/2}\right]$$

α angle of attack or slope of streamline surface

$\bar{\alpha}$ amplitude of angle of attack $\left(\dot{h}_{max}/U\right)$

$\beta = \sqrt{M^2 - 1}$

Λ sweepback angle

γ_1 constant $\left(\frac{1}{\beta - k}\right)$

γ_2 constant $\left(\frac{1}{\beta + k}\right)$

γ_3 constant $\left(\frac{2k}{\beta + k}\right)$

$\delta = \frac{M}{\beta}(x + \beta y)$

ζ source location along z-axis

η source location along y-axis

λ slope of diaphragm

$\bar{\lambda}$ amplitude of oscillation on diaphragm

$\mu = \xi' - x'$

ξ source location along x-axis (t-axis)

σ_B slope of bottom wing surface

σ_T slope of top wing surface

$\sigma_{m,n}$ coefficients for C_p

τ time interval

$\tau_1 = \frac{M}{a\beta^2}(x - \xi) - \frac{r}{a}$

$\tau_2 = \frac{M}{a\beta^2}(x - \xi) + \frac{r}{a}$

ϕ perturbation velocity potential

ω angular velocity per second

$\bar{\omega}$ frequency parameter $\left(\frac{\omega Mc}{a\beta}\right)$

$\bar{\bar{\omega}}$ frequency parameter $\left(\frac{\omega Mc}{a\beta^2}\right)$

Subscripts:

B bottom wing surface

D diaphragm, except in the case of drag coefficient C_D

I imaginary part

R real part

T top wing surface

w wing

APPENDIX B

FORMULAS USED IN SECOND METHOD

Formulas for Use with Equation (49)

$$e_2 = 4 - 4i\bar{\omega}\gamma_2(x - ky) - 2\bar{\omega}^2\gamma_2{}^2(x - ky)^2 + \frac{2}{3}i\bar{\omega}^3\gamma_2{}^3(x - ky)^3 + \frac{1}{6}\bar{\omega}^4\gamma_2{}^4(x - ky)^4$$

$$e_4 = \frac{\gamma_{31}}{M}\frac{\gamma_2}{\gamma_1}\left[-4i\bar{\omega} - 4\bar{\omega}^2\gamma_2(x - ky) + 2i\bar{\omega}^3\gamma_2{}^2(x - ky)^2 + \frac{2}{3}\bar{\omega}^4\gamma_2{}^3(x - ky)^3\right]$$

$$e_6 = \frac{\gamma_{32}}{M^2}\left(\frac{\gamma_2}{\gamma_1}\right)^2\left[-2\bar{\omega}^2 + 2i\bar{\omega}^3\gamma_2(x - ky) + \bar{\omega}^4\gamma_2{}^2(x - ky)^2\right]$$

$$e_8 = \frac{\gamma_{33}}{M^3}\left(\frac{\gamma_2}{\gamma_1}\right)^3\left[\frac{2}{3}i\bar{\omega}^3 + \frac{2}{3}\bar{\omega}^4\gamma_2(x - ky)\right]$$

$$e_{10} = \frac{\gamma_{34}}{M^4}\left(\frac{\gamma_2}{\gamma_1}\right)^4\frac{1}{3}\bar{\omega}^4$$

$$g_4 = \frac{4}{M^4}\left(\frac{\gamma_2}{\gamma_1}\right)^{1/2}\bar{\omega}^2\left[-\frac{2}{3} + \frac{2}{3}i\bar{\omega}\gamma_2(x - ky) + \frac{1}{3}\bar{\omega}^2\gamma_2{}^2(x - ky)^2\right]$$

$$g_6 = \frac{4}{M^4}\left(\frac{\gamma_2}{\gamma_1}\right)^{3/2}i\bar{\omega}^3\left[\frac{2}{3} - \frac{2}{3}i\bar{\omega}\gamma_2(x - ky)\right]\frac{\overline{\gamma}_{31}}{M}$$

$$g_8 = \frac{4}{M^4}\left(\frac{\gamma_2}{\gamma_1}\right)^{5/2}\bar{\omega}^4\frac{1}{3}\frac{\overline{\gamma}_{32}}{M^2}$$

$$h_6 = \frac{8}{M^8}\left(\frac{\gamma_2}{\gamma_1}\right)^{3/2}\bar{\omega}^4\left(\frac{1}{15}\right)$$

where

$$\bar{\omega} = \frac{\omega M c}{a\beta}$$

$$\gamma_3 = \frac{2k}{\beta + k} = 2k\gamma_2$$

$$\gamma_{31} = \frac{\gamma_1}{\gamma_2}\left(\gamma_3 - \frac{2}{3}\right)$$

$$\gamma_{32} = \left(\frac{\gamma_1}{\gamma_2}\right)^2\left(\gamma_3^2 - \frac{4}{3}\gamma_3 + \frac{8}{15}\right)$$

$$\gamma_{33} = \left(\frac{\gamma_1}{\gamma_2}\right)^3\left(\gamma_3^3 - 2\gamma_3^2 + \frac{8}{5}\gamma_3 - \frac{16}{35}\right)$$

$$\gamma_{34} = \left(\frac{\gamma_1}{\gamma_2}\right)^4\left(\frac{1}{2}\gamma_3^4 - \frac{4}{3}\gamma_3^3 + \frac{8}{5}\gamma_3^2 - \frac{32}{35}\gamma_3 + \frac{64}{315}\right)$$

$$\bar{\gamma}_{31} = \frac{\gamma_1}{\gamma_2}\left(\gamma_3 - \frac{2}{5}\right)$$

$$\bar{\gamma}_{32} = \left(\frac{\gamma_1}{\gamma_2}\right)^2\left(\gamma_3^2 - \frac{4}{5}\gamma_3 + \frac{8}{35}\right)$$

Formulas for Use with Equations (50) and (53)

$$\sigma_{1,1} = 2(\gamma_1\gamma_2)^{1/2}(2)$$

$$\sigma_{1,2} = 2(\gamma_1\gamma_2)^{1/2} i\bar{\omega}\gamma_2\left(-2 - \frac{3}{2}\gamma_{31}\right)$$

$$\sigma_{1,3} = 2(\gamma_1\gamma_2)^{1/2}\bar{\omega}^2\gamma_2^2\left(-1 - \frac{3}{2}\gamma_{31} - \frac{5}{8}\gamma_{32} - \frac{1}{6}\frac{1}{M^2}\frac{\gamma_1}{\gamma_2}\right)$$

$$\sigma_{1,4} = 2(\gamma_1\gamma_2)^{1/2} i\bar{\omega}^3\gamma_2^3\left(\frac{1}{3} + \frac{3}{4}\gamma_{31} + \frac{5}{8}\gamma_{32} + \frac{35}{192}\gamma_{33} + \frac{1}{6M^2}\frac{\gamma_1}{\gamma_2} + \frac{5}{48}\frac{1}{M^2}\frac{\gamma_1}{\gamma_2}\bar{\gamma}_{31}\right)$$

$$\sigma_{1,5} = 2(\gamma_1\gamma_2)^{1/2}\bar{\omega}^4\gamma_2^4\left[\frac{1}{12} + \frac{1}{4}\gamma_{31} + \frac{5}{16}\gamma_{32} + \frac{35}{192}\gamma_{33} + \frac{21}{256}\gamma_{34} + \frac{1}{12M^2}\frac{\gamma_1}{\gamma_2} + \frac{5}{48}\frac{1}{M^2}\frac{\gamma_1}{\gamma_2}\bar{\gamma}_{31} + \frac{7}{192}\frac{1}{M^2}\frac{\gamma_1}{\gamma_2}\bar{\gamma}_{32} + \frac{1}{160M^4}\left(\frac{\gamma_1}{\gamma_2}\right)^2\right]$$

$$\sigma_{2,0} = 2(\gamma_1)^{1/2}(-2)$$

$$\sigma_{2,1} = 2(\gamma_1)^{1/2}i\bar{\omega}\gamma_2\left(2 + \frac{3}{2}\gamma_{31}\right)$$

$$\sigma_{2,2} = 2(\gamma_1)^{1/2}\bar{\omega}^2\gamma_2^2\left(1 + \frac{3}{2}\gamma_{31} + \frac{5}{8}\gamma_{32} - \frac{1}{6M^2}\frac{\gamma_1}{\gamma_2}\right)$$

$$\sigma_{2,3} = 2(\gamma_1)^{1/2}i\bar{\omega}^3\gamma_2^3\left(-\frac{1}{3} - \frac{3}{4}\gamma_{31} - \frac{5}{8}\gamma_{32} - \frac{35}{192}\gamma_{33} + \frac{1}{6M^2}\frac{\gamma_1}{\gamma_2} + \frac{5}{48}\frac{1}{M^2}\frac{\gamma_1}{\gamma_2}\bar{\gamma}_{31}\right)$$

$$\sigma_{2,4} = 2(\gamma_1)^{1/2}\bar{\omega}^4\gamma_2^4\left[-\frac{1}{12} - \frac{1}{4}\gamma_{31} - \frac{5}{16}\gamma_{32} - \frac{35}{192}\gamma_{33} - \frac{21}{256}\gamma_{34} + \frac{1}{12M^2}\frac{\gamma_1}{\gamma_2} + \frac{5}{48M^2}\frac{\gamma_1}{\gamma_2}\bar{\gamma}_{31} + \frac{7}{192}\frac{1}{M^2}\frac{\gamma_1}{\gamma_2}\bar{\gamma}_{32} + \frac{1}{160M^4}\left(\frac{\gamma_1}{\gamma_2}\right)^2\right]$$

$$\sigma_{3,0} = 2(\gamma_1)^{1/2}i\bar{\omega}\gamma_2(\gamma_{31})$$

$$\sigma_{3,1} = 2(\gamma_1)^{1/2}\bar{\omega}^2\gamma_2^2\left(\gamma_{31} + \frac{5}{12}\gamma_{32}\right)$$

$$\sigma_{3,2} = 2(\gamma_1)^{1/2}i\bar{\omega}^3\gamma_2^3\left(-\frac{1}{2}\gamma_{31} - \frac{5}{12}\gamma_{32} - \frac{35}{288}\gamma_{33}\right)$$

$$\sigma_{3,3} = 2(\gamma_1)^{1/2}\bar{\omega}^4\gamma_2^4\left(-\frac{1}{6}\gamma_{31} - \frac{5}{24}\gamma_{32} - \frac{35}{288}\gamma_{33} - \frac{7}{128}\gamma_{34}\right)$$

$$\sigma_{4,0} = 2(\gamma_1)^{1/2}\bar{\omega}^2\gamma_2^2\left(\frac{1}{3}\gamma_{32}\right)$$

$$\sigma_{4,1} = 2(\gamma)^{1/2}i\bar{\omega}^3\gamma_2^3\left(-\frac{1}{3}\gamma_{32} - \frac{7}{72}\gamma_{33}\right)$$

$$\sigma_{4,2} = 2(\gamma)^{1/2}\bar{\omega}^4\gamma_2^4\left(-\frac{1}{6}\gamma_{32} - \frac{7}{72}\gamma_{33} - \frac{7}{160}\gamma_{34}\right)$$

$$\sigma_{5,0} = 2(\gamma)^{1/2} i\bar{\omega}^3 \gamma_2{}^3 \left(-\frac{1}{12}\gamma_{33}\right)$$

$$\sigma_{5,1} = 2(\gamma)^{1/2} \bar{\omega}^4 \gamma_2{}^4 \left(-\frac{1}{12}\gamma_{33} - \frac{3}{80}\gamma_{34}\right)$$

$$\sigma_{6,0} = 2(\gamma)^{1/2} \bar{\omega}^4 \gamma_2{}^4 \left(-\frac{1}{30}\gamma_{34}\right)$$

$$\sigma_{7,1} = 2(\gamma_1)^{3/2} \frac{1}{M^2} \bar{\omega}^2 \left(\frac{1}{3}\right)$$

$$\sigma_{7,2} = 2(\gamma_1)^{3/2} \frac{\gamma_2}{M^2} i\bar{\omega}^3 \left(-\frac{1}{3} - \frac{5}{24}\bar{\gamma}_{31}\right)$$

$$\sigma_{7,3} = 2(\gamma_1)^{3/2} \frac{\gamma_2{}^2}{M^2} \bar{\omega}^4 \left(-\frac{1}{6} - \frac{5}{24}\bar{\gamma}_{31} - \frac{7}{96}\bar{\gamma}_{32} - \frac{1}{80}\frac{1}{M^2}\frac{\gamma_1}{\gamma_2}\right)$$

$$\sigma_{8,0} = 2(\gamma_1)^{3/2} \frac{1}{M^2} \bar{\omega}^2 \left(\frac{4}{9}\right)$$

$$\sigma_{8,1} = 2(\gamma_1)^{3/2} \frac{\gamma_2}{M^2} \left(-\frac{4}{9} - \frac{5}{18}\bar{\gamma}_{31}\right) i\bar{\omega}^3$$

$$\sigma_{8,2} = 2(\gamma_1)^{3/2} \frac{\gamma_2{}^2}{M^2} \bar{\omega}^4 \left(-\frac{2}{9} - \frac{5}{18}\bar{\gamma}_{31} - \frac{7}{72}\bar{\gamma}_{32} - \frac{1}{60}\frac{1}{M^2}\frac{\gamma_1}{\gamma_2}\right)$$

$$\sigma_{9,0} = 2(\gamma_1)^{3/2} \frac{\gamma_2}{M^2} i\bar{\omega}^3 \left(-\frac{1}{3}\bar{\gamma}_{31}\right)$$

$$\sigma_{9,1} = 2(\gamma_1)^{3/2} \frac{\gamma_2{}^2}{M^2} \bar{\omega}^4 \left(-\frac{1}{3}\bar{\gamma}_{31} - \frac{7}{60}\bar{\gamma}_{32} - \frac{1}{50}\frac{1}{M^2}\frac{\gamma_1}{\gamma_2}\right)$$

$$\sigma_{10,0} = 2(\gamma_1)^{3/2} \frac{\gamma_2{}^2}{M^2} \bar{\omega}^4 \left(-\frac{2}{15}\bar{\gamma}_{32} + \frac{4}{75}\frac{1}{M^2}\frac{\gamma_1}{\gamma_2}\right)$$

$$\overline{\sigma_{2,1}} = 2(\gamma_1)^{1/2} \bar{\omega}^2 \frac{\gamma_2{}^2}{M^2} \left(-\frac{1}{6}\frac{\gamma_1}{\gamma_2}\right)$$

$$\overline{\sigma_{2,2}} = 2(\gamma_1)^{1/2} i\bar{\omega}^3 \frac{\gamma_2^3}{M^2}\left(\frac{1}{6}\frac{\gamma_1}{\gamma_2} + \frac{5}{48}\frac{\gamma_1}{\gamma_2}\bar{\gamma}_{31}\right)$$

$$\overline{\sigma_{2,3}} = 2(\gamma_1)^{1/2} \bar{\omega}^4 \frac{\gamma_2^4}{M^2}\left[\frac{1}{12}\frac{\gamma_1}{\gamma_2} + \frac{5}{48}\frac{\gamma_1}{\gamma_2}\bar{\gamma}_{31} + \frac{7}{192}\frac{\gamma_1}{\gamma_2}\bar{\gamma}_{32} + \frac{1}{160}\frac{1}{M^2}\left(\frac{\gamma_1}{\gamma_2}\right)^2\right]$$

Formulas for Use with Equation (55)

$$a_0 = \sigma_{1,1}$$

$$a_1 = \frac{i\omega}{U}\sigma_{1,1} + 2\sigma_{1,2}$$

$$a_2 = \frac{i\omega}{U}\sigma_{1,2} + 3\sigma_{1,3}$$

$$a_3 = \frac{i\omega}{U}\sigma_{1,3} + 4\sigma_{1,4}$$

$$a_4 = \frac{i\omega}{U}\sigma_{1,4} + 5\sigma_{1,5}$$

$$a_5 = \frac{i\omega}{U}\sigma_{1,5}$$

$$b_0 = \sigma_{2,1} + \frac{i\omega}{U}\sigma_{2,0} + \frac{3}{2}\sigma_{3,0}$$

$$b_1 = 2\sigma_{2,2} + \frac{i\omega}{U}\sigma_{2,1} + \frac{3}{2}\sigma_{3,1} + \overline{\sigma_{2,1}}$$

$$b_2 = 3\sigma_{2,3} + \frac{i\omega}{U}\sigma_{2,2} + \frac{3}{2}\sigma_{3,2} + \overline{\sigma_{2,2}}$$

$$b_3 = 4\sigma_{2,4} + \frac{i\omega}{U}\sigma_{2,3} + \frac{3}{2}\sigma_{3,3} + \overline{\sigma_{2,3}}$$

$$b_4 = \frac{i\omega}{U}\sigma_{2,4}$$

$$c_0 = \sigma_{3,1} + \frac{i\omega}{U}\sigma_{3,0} + \frac{5}{2}\sigma_{4,0}$$

$$c_1 = 2\sigma_{3,2} + \frac{i\omega}{U}\sigma_{3,1} + \frac{5}{2}\sigma_{4,1}$$

$$c_2 = 3\sigma_{3,3} + \frac{i\omega}{U}\sigma_{3,2} + \frac{5}{2}\sigma_{4,2}$$

$$c_3 = \frac{i\omega}{U}\sigma_{3,3}$$

$$d_0 = \sigma_{4,1} + \frac{i\omega}{U}\sigma_{4,0} + \frac{7}{2}\sigma_{5,0}$$

$$d_1 = 2\sigma_{4,2} + \frac{i\omega}{U}\sigma_{4,1} + \frac{7}{2}\sigma_{5,1}$$

$$d_2 = \frac{i\omega}{U}\sigma_{4,2}$$

$$e_0 = \sigma_{5,1} + \frac{i\omega}{U}\sigma_{5,0} + \frac{9}{2}\sigma_{6,0}$$

$$e_1 = \frac{i\omega}{U}\sigma_{5,1}$$

$$f = \frac{i\omega}{U}\sigma_{6,0}$$

$$g_0 = \sigma_{7,1} + \frac{3}{2}\sigma_{8,0}$$

$$g_1 = 2\sigma_{7,2} + \frac{i\omega}{U}\sigma_{7,1} + \frac{3}{2}\sigma_{8,1}$$

$$g_2 = 3\sigma_{7,3} + \frac{i\omega}{U}\sigma_{7,2} + \frac{3}{2}\sigma_{8,2}$$

$$g_3 = \frac{i\omega}{U}\sigma_{7,3}$$

$$h_0 = \sigma_{8,1} + \frac{i\omega}{U}\sigma_{8,0} + \frac{5}{2}\sigma_{9,0}$$

$$h_1 = \frac{i\omega}{U}\sigma_{8,1} + 2\sigma_{8,2} + \frac{5}{2}\sigma_{9,1}$$

$$h_2 = \frac{i\omega}{U}\sigma_{8,2}$$

$$i_0 = \sigma_{9,1} + \frac{i\omega}{U}\sigma_{9,0} + \frac{7}{2}\sigma_{10,0}$$

$$i_1 = \frac{i\omega}{U}\sigma_{9,1}$$

$$j = \sigma_{10,0}\frac{i\omega}{U}$$

Formulas for Use with Equation (55); $\bar{\bar{\omega}} = \frac{\bar{\omega}}{\beta} = \frac{\omega Mc}{a\beta^2}$

$$\sigma_{1,1} = \frac{4}{\beta}$$

$$\sigma_{1,2} = \frac{1}{\beta}\bar{\bar{\omega}}(-2i)$$

$$\sigma_{1,3} = \frac{1}{\beta}\bar{\bar{\omega}}^2\left(-\frac{2}{3} - \frac{1}{3M^2}\right)$$

$$\sigma_{1,4} = \frac{1}{\beta}i\bar{\bar{\omega}}^3\left(\frac{1}{6} + \frac{1}{4M^2}\right)$$

$$\sigma_{1,5} = \frac{1}{\beta}\bar{\bar{\omega}}^4\left(\frac{1}{30} + \frac{1}{10M^2} + \frac{1}{80M^4}\right)$$

$$\sigma_{2,0} = \beta^{-1/2}(-4)$$

$$\sigma_{2,1} = \beta^{-1/2}\, i\bar{\bar{\omega}}(2)$$

$$\sigma_{2,2} = \beta^{-1/2}\,\bar{\bar{\omega}}^2\left(\frac{2}{3} - \frac{1}{3M^2}\right)$$

$$\sigma_{2,3} = \beta^{-1/2}\, i\bar{\bar{\omega}}^3\left(-\frac{1}{6} + \frac{1}{4M^2}\right)$$

$$\sigma_{2,4} = \beta^{-1/2}\,\bar{\bar{\omega}}^4\left(-\frac{1}{30} + \frac{1}{10M^2} + \frac{1}{80M^4}\right)$$

$$\sigma_{3,0} = \beta^{-1/2}\, i\bar{\bar{\omega}}\left(-\frac{4}{3}\right)$$

$$\sigma_{3,1} = \beta^{-1/2}\,\bar{\bar{\omega}}^{2}\left(-\frac{8}{9}\right)$$

$$\sigma_{3,2} = \beta^{-1/2}\,i\bar{\bar{\omega}}^{3}\left(\frac{1}{3}\right)$$

$$\sigma_{3,3} = \beta^{-1/2}\,\bar{\bar{\omega}}^{4}\left(\frac{4}{45}\right)$$

$$\sigma_{4,0} = \beta^{-1/2}\,\bar{\bar{\omega}}^{2}\left(\frac{16}{45}\right)$$

$$\sigma_{4,1} = \beta^{-1/2}\,i\bar{\bar{\omega}}^{3}\left(-\frac{4}{15}\right)$$

$$\sigma_{4,2} = \beta^{-1/2}\,\bar{\bar{\omega}}^{4}\left(-\frac{8}{75}\right)$$

$$\sigma_{5,0} = \beta^{-1/2}\,i\bar{\bar{\omega}}^{3}\left(\frac{8}{105}\right)$$

$$\sigma_{5,1} = \beta^{-1/2}\,\bar{\bar{\omega}}^{4}\left(\frac{32}{525}\right)$$

$$\sigma_{6,0} = \beta^{-1/2}\,\bar{\bar{\omega}}^{4}\left(\frac{-64}{4725}\right)$$

$$\sigma_{7,1} = \beta^{1/2}\,\frac{1}{M^2}\,\bar{\bar{\omega}}^{2}\left(\frac{2}{3}\right)$$

$$\sigma_{7,2} = \beta^{1/2}\,\frac{1}{M^2}\,i\bar{\bar{\omega}}^{3}\left(-\frac{1}{2}\right)$$

$$\sigma_{7,3} = \beta^{1/2}\,\frac{1}{M^2}\,\bar{\bar{\omega}}^{4}\left(-\frac{1}{5} - \frac{1}{40M^2}\right)$$

$$\sigma_{8,0} = \beta^{1/2}\,\frac{1}{M^2}\,\bar{\bar{\omega}}^{2}\left(\frac{8}{9}\right)$$

$$\sigma_{8,1} = \beta^{1/2}\,\frac{1}{M^2}\,i\bar{\bar{\omega}}^{3}\left(-\frac{2}{3}\right)$$

$$\sigma_{8,2} = \beta^{1/2}\,\frac{1}{M^2}\,\bar{\bar{\omega}}^{4}\left(-\frac{4}{15} - \frac{1}{30M^2}\right)$$

$$\sigma_{9,0} = \beta^{1/2} \frac{1}{M^2} i\bar{\bar{\omega}}^3\left(\frac{4}{15}\right)$$

$$\sigma_{9,1} = \beta^{1/2} \frac{1}{M^2} \bar{\bar{\omega}}^4\left(\frac{16}{75} - \frac{1}{25M^2}\right)$$

$$\sigma_{10,0} = \beta^{1/2} \frac{1}{M^2} \bar{\bar{\omega}}^4\left(\frac{-32}{525} + \frac{8}{75M^2}\right)$$

$$\overline{\sigma_{2,1}} = \beta^{-1/2} \frac{1}{M^2} \bar{\bar{\omega}}^2\left(-\frac{1}{3}\right)$$

$$\overline{\sigma_{2,2}} = \beta^{-1/2} \frac{1}{M^2} i\bar{\bar{\omega}}^3\left(\frac{1}{4}\right)$$

$$\overline{\sigma_{2,3}} = \beta^{-1/2} \frac{1}{M^2} \bar{\bar{\omega}}^4\left(\frac{1}{10} + \frac{1}{80M^2}\right)$$

Formulas for Use with Equations (58) and (59)

$$b_0' = 0$$

$$b_1' = \frac{1}{\beta} 2 \frac{i\omega}{U}$$

$$b_2' = \frac{1}{\beta} \frac{\omega}{U}\left(\frac{2}{3} \bar{\bar{\omega}}\right)$$

$$b_3' = \frac{-1}{\beta} \frac{i\omega}{U} \bar{\bar{\omega}}^2\left(\frac{1}{6} + \frac{1}{12M^2}\right)$$

$$b_4' = \frac{-1}{\beta} \frac{\omega}{U} \bar{\bar{\omega}}^3\left(\frac{1}{30} + \frac{1}{20M^2}\right)$$

$$b_5' = \frac{1}{\beta} \frac{\omega}{U}\left(\bar{\bar{\omega}}^4\right)\left(\frac{1}{180} + \frac{1}{60M^2} + \frac{1}{480M^4}\right)$$

$$c_0' = \frac{1}{2\beta^2}$$

$$c_1' = \frac{i}{\beta^2}\bar{\omega}\left(-\frac{1}{3} + \frac{1}{2}\frac{\beta^2}{M^2}\right)$$

$$c_2' = \frac{1}{\beta^2}\bar{\omega}^2\left(-\frac{1}{8} + \frac{1}{6}\frac{\beta^2}{M^2} - \frac{1}{16M^2}\right)$$

$$c_3' = \frac{i}{\beta^2}\bar{\omega}^3\left(\frac{1}{30} - \frac{1}{24}\frac{\beta^2}{M^2} + \frac{1}{20M^2} - \frac{1}{48}\frac{\beta^2}{M^2}\right)$$

$$c_4' = \frac{1}{\beta^2}\bar{\omega}^4\left(\frac{1}{144} - \frac{1}{120}\frac{\beta^2}{M^2} + \frac{1}{48M^2} - \frac{1}{80}\frac{\beta^2}{M^2} + \frac{1}{384M^4}\right)$$

$$c_5' = \frac{i}{\beta^2}\bar{\omega}^5\left(\frac{1}{720}\frac{\beta^2}{M^2} + \frac{1}{240}\frac{\beta^2}{M^4} + \frac{1}{1920}\frac{\beta^2}{M^6}\right)$$

APPENDIX C

INTEGRALS USED IN SECOND METHOD

$$\int \frac{x^{2n}\,dx}{(a^2 - x^2)^{1/2}} = -(a^2 - x^2)^{1/2} \sum_{r=1}^{n} \frac{1}{4^{r-1}} \frac{(2n - 1)!(n - r + 1)!(n - r)!}{(2n - 2r + 2)!n!(n - 1)!}\, a^{2(r-1)} x^{2n-2r+1} +$$

$$\frac{1}{4^{n-1}} \frac{(2n - 1)!}{2(n!)(n - 1)!}\, a^{2n} \sin^{-1} \frac{x}{a} \qquad (n \geqq 1) \qquad (C1)$$

$$\int x^{2n}(a^2 - x^2)^{1/2}\,dx = -(a^2 - x^2)^{3/2} \sum_{r=1}^{n} \frac{1}{4^{r-1}} \frac{(2n-1)!(n-r+1)!(n-r+1)!}{(2n-2r+2)!(n+1)!(n-1)!}\, a^{2(r-1)} x^{2n-2r+1} +$$

$$\frac{1}{4^n} \frac{(2n-1)!a^{2n}}{(n+1)!(n-1)!}\left[x(a^2 - x^2)^{1/2} + a^2 \sin^{-1} \frac{x}{a}\right] \qquad (n \geqq 1) \qquad (C2)$$

$$\int \frac{d\eta}{\eta^{1/2}} (\mu + \eta) = 2\eta^{1/2}(\mu + \eta) - \frac{4}{3}\eta^{3/2} \qquad (C3)$$

$$\int \frac{d\eta}{\eta^{1/2}} (\mu + \eta)^2 = 2\eta^{1/2}(\mu + \eta)^2 - \frac{8}{3} \eta^{3/2}(\mu + \eta) + \frac{16}{15} \eta^{5/2} \quad (C4)$$

$$\int \frac{d\eta}{\eta^{1/2}} (\mu + \eta)^3 = 2\eta^{1/2}(\mu + \eta)^3 - 4\eta^{3/2}(\mu + \eta)^2 + \frac{16}{5} \eta^{5/2}(\mu + \eta) - \frac{32}{35} \eta^{7/2} \quad (C5)$$

$$\int \frac{d\eta}{\eta^{1/2}} (\mu + \eta)^4 = 2\eta^{1/2}(\mu + \eta)^4 - \frac{16}{3} \eta^{3/2}(\mu + \eta)^3 + \frac{32}{5} \eta^{5/2}(\mu + \eta)^2 - \frac{128}{35} \eta^{7/2}(\mu + \eta) + \frac{256}{315} \eta^{9/2} \quad (C6)$$

$$\int d\eta\, \eta^{1/2}(\mu + \eta) = \frac{2}{3} \eta^{3/2}(\mu + \eta) - \frac{4}{15} \eta^{5/2} \quad (C7)$$

$$\int d\eta\, \eta^{1/2}(\mu + \eta)^2 = \frac{2}{3} \eta^{3/2}(\mu + \eta)^2 - \frac{8}{15} \eta^{5/2}(\mu + \eta) + \frac{16}{105} \eta^{7/2} \quad (C8)$$

REFERENCES

1. Garrick, I. E., and Rubinow, S. I.: Theoretical Study of Air Forces on an Oscillating or Steady Thin Wing in a Supersonic Main Stream. NACA Rep. 872, 1947. (Formerly NACA TN 1383.)

2. Evvard, John C.: A Linearized Solution for Time-Dependent Velocity Potentials near Three-Dimensional Wings at Supersonic Speeds. NACA TN 1699, 1948.

3. Miles, John W.: The Oscillating Rectangular Airfoil at Supersonic Speeds. NAVORD Rep. 1170 (NOTS 226), U.S. Naval Ordnance Test Station, July 21, 1949.

4. Baker, Bevan B., and Copson, E. T.: The Mathematical Theory of Huygen's Principle. The Clarendon Press (Oxford), 1939.

5. Chang, Chieh-Chien: The Transient Reaction of an Airfoil Due to Change in Angle of Attack at Supersonic Speed. Jour. Aero. Sci., vol. 15, no. 11, Nov. 1948, pp. 635-655.

6. Chang, Chieh-Chien: Transient Aerodynamic Behavior of an Airfoil Due to Different Arbitrary Modes of Nonstationary Motions in a Supersonic Flow. NACA TN 2333, 1951.

7. Garrick, I. E., and Rubinow, S. I.: Flutter and Oscillating Air-Force Calculations for an Airfoil in a Two-Dimensional Supersonic Flow. NACA TN 1158, 1946.

8. Miles, John W.: Harmonic and Transient Motion of a Swept Wing in Supersonic Flow. Jour. Aero. Sci., vol. 15, no. 6, June 1948, pp. 343-346, 370.

9. Evvard, John C.: Distribution of Wave Drag and Lift in the Vicinity of Wing Tips at Supersonic Speeds. NACA TN 1382, 1947.

10. Watson, G. N.: A Treatise on the Theory of Bessel Functions. Second ed., The Macmillan Co., 1944.

11. Jahnke, E., and Emde F.: Tables of Functions with Formulae and Curves. Dover Publications, 1943.

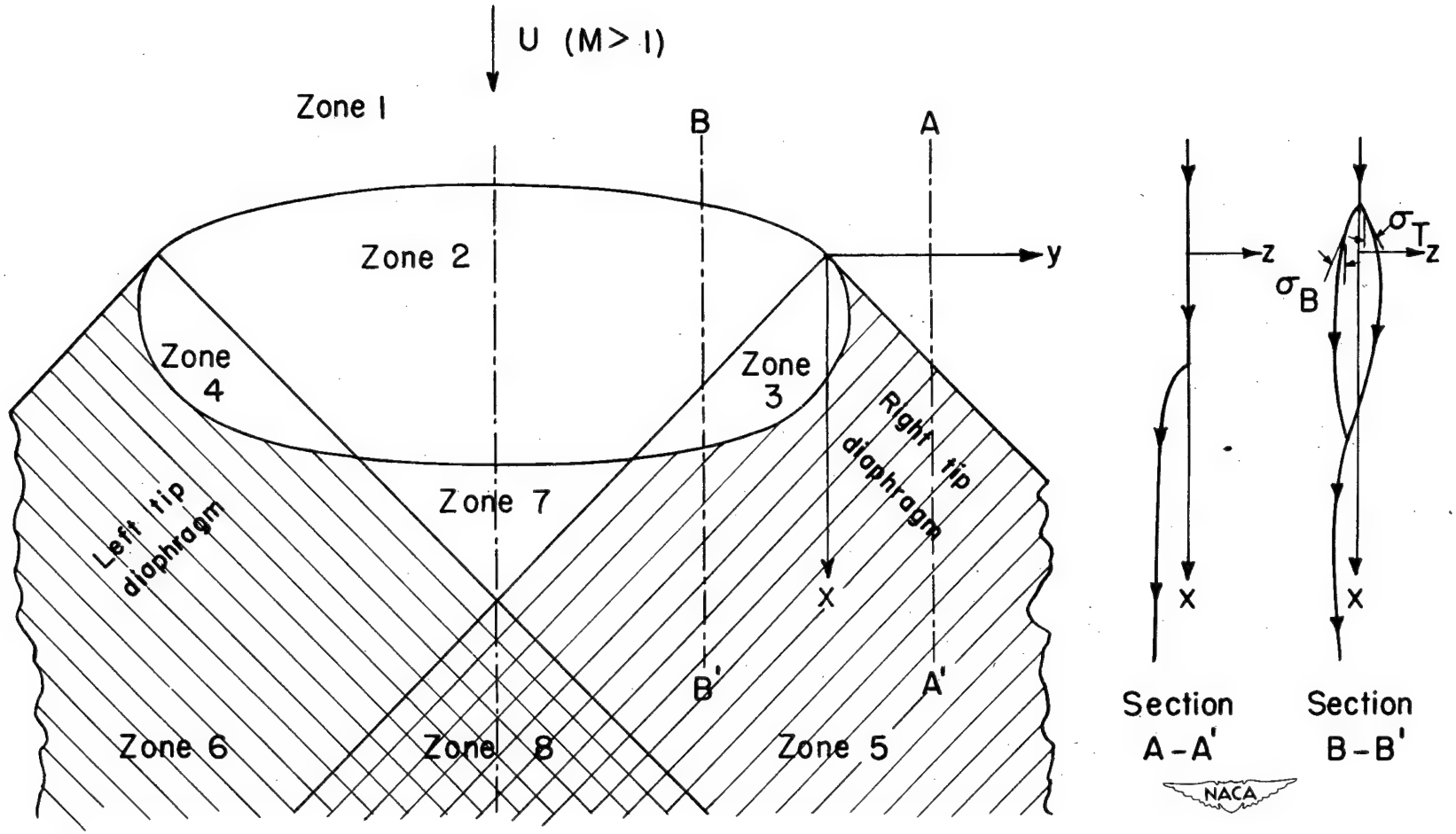

Figure 1.- Division into zones of streamline surface of a wing and its tip diaphragms in supersonic flow.

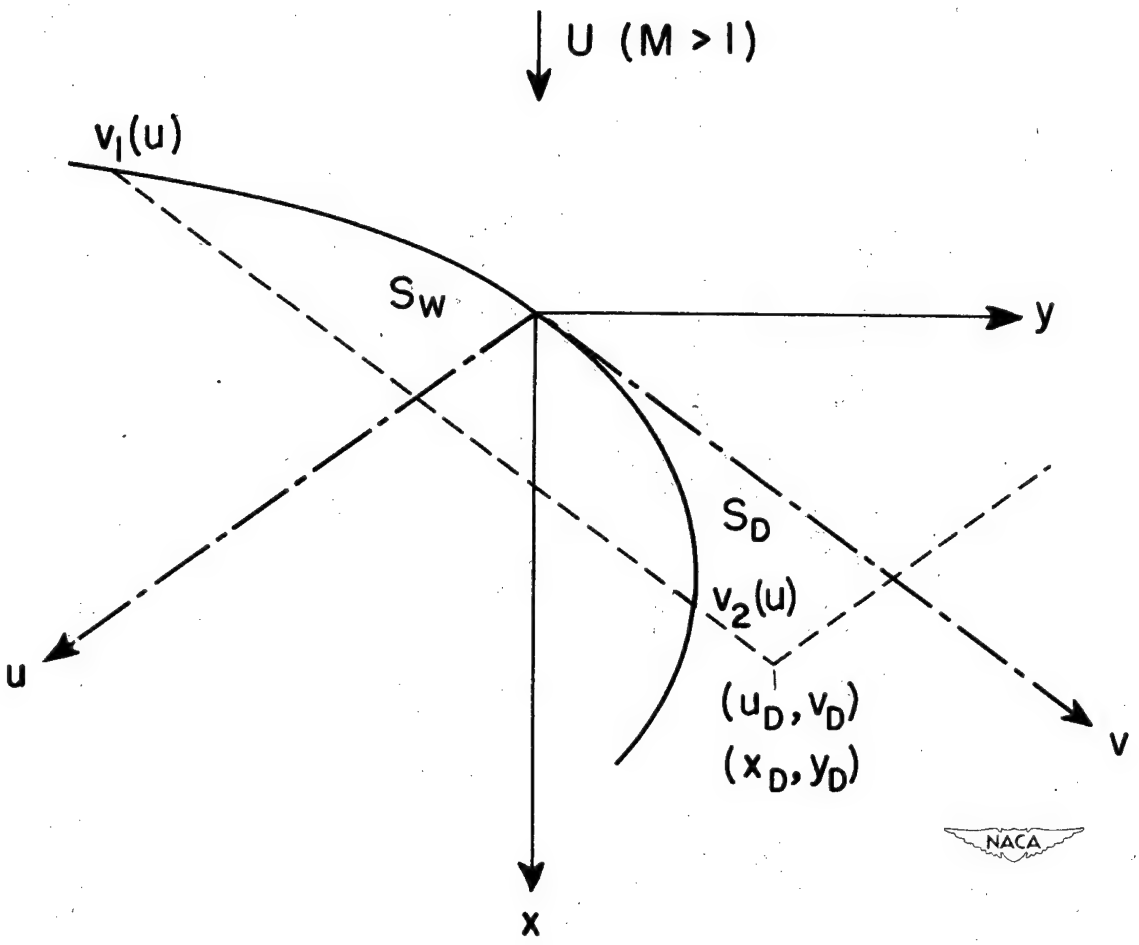

Figure 2.- Wing area S_w and diaphragm area S_D which lie in forward Mach cone of a point (x_D, y_D) on right tip diaphragm.

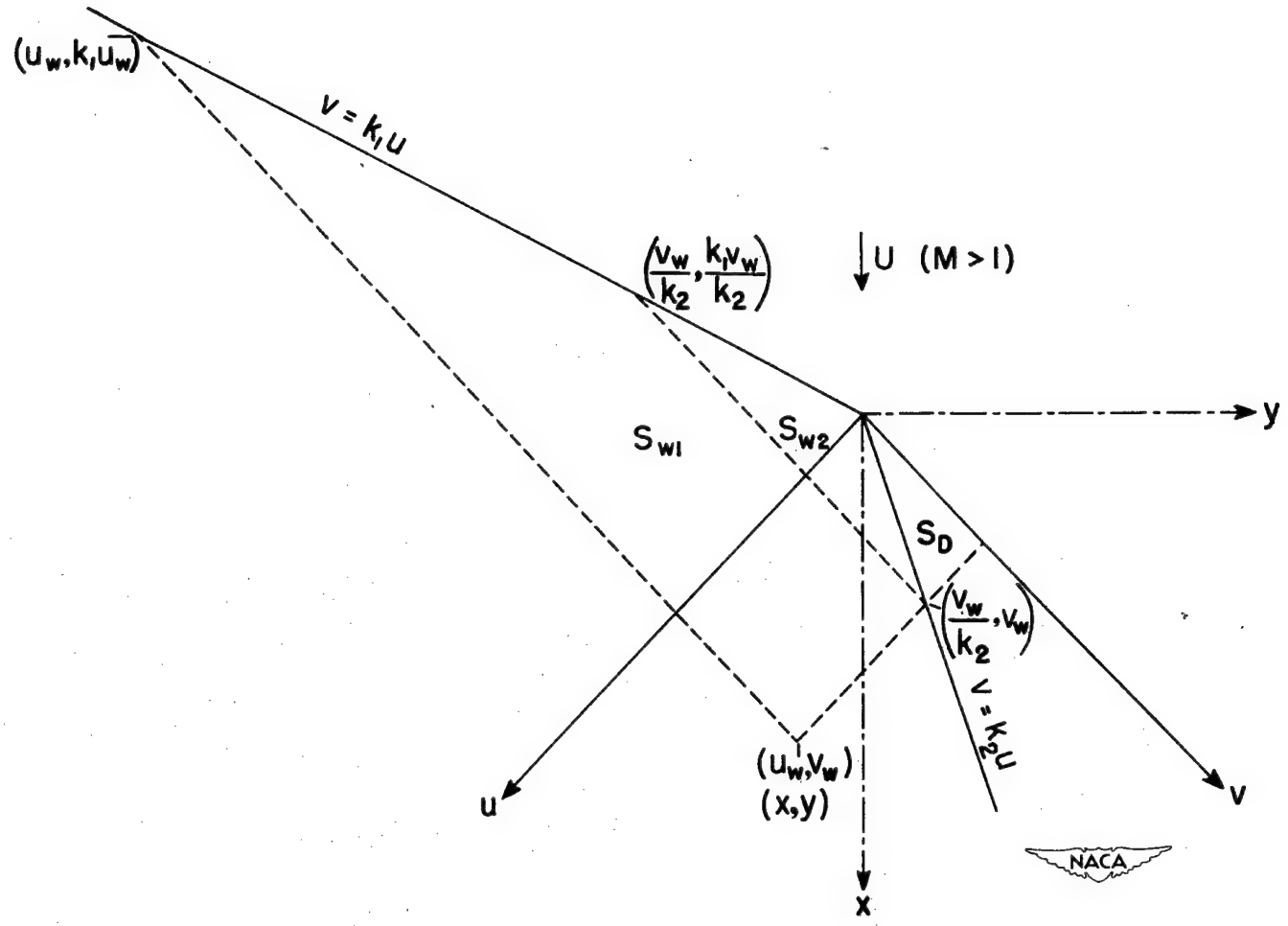

Figure 3.- Wing areas S_{w1} and S_{w2} and diaphragm area S_D which lie in forward Mach cone of a point (x,y) on wing surface. Two coordinate systems (x,y) and (u,v) shown.

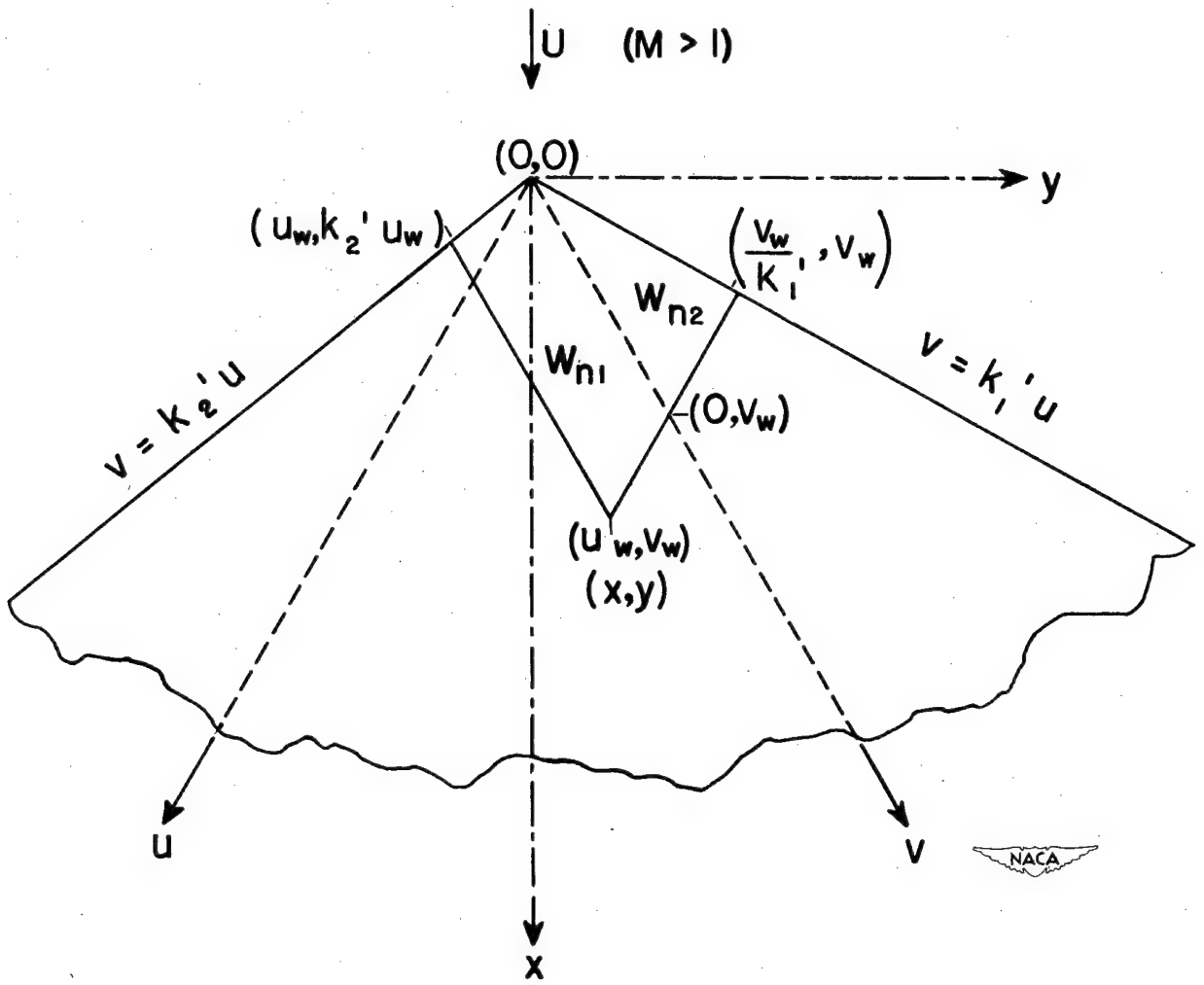

Figure 4.- Wing areas W_{n1} and W_{n2} which lie in forward Mach cone of a point (x,y) in nose section of a wing with supersonic leading edge. Two coordinate systems (x,y) and (u,v) shown.

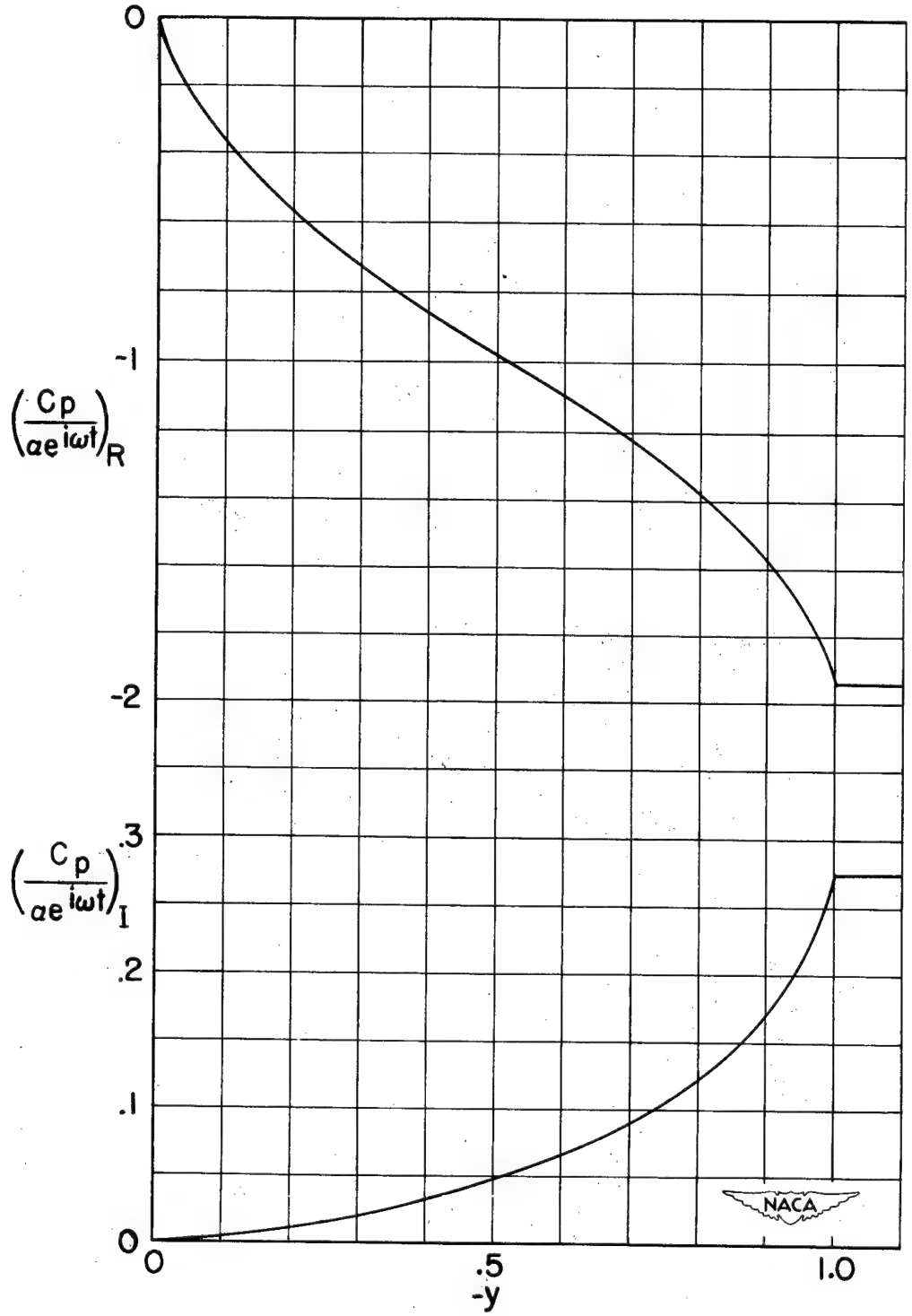

Figure 5.- Pressure distribution along trailing edge of a rectangular wing of unit chord with $\frac{\omega c}{a} = 0.2$, $M = \sqrt{2}$, and $x = 1$. Calculated with first method (Fresnal integral).

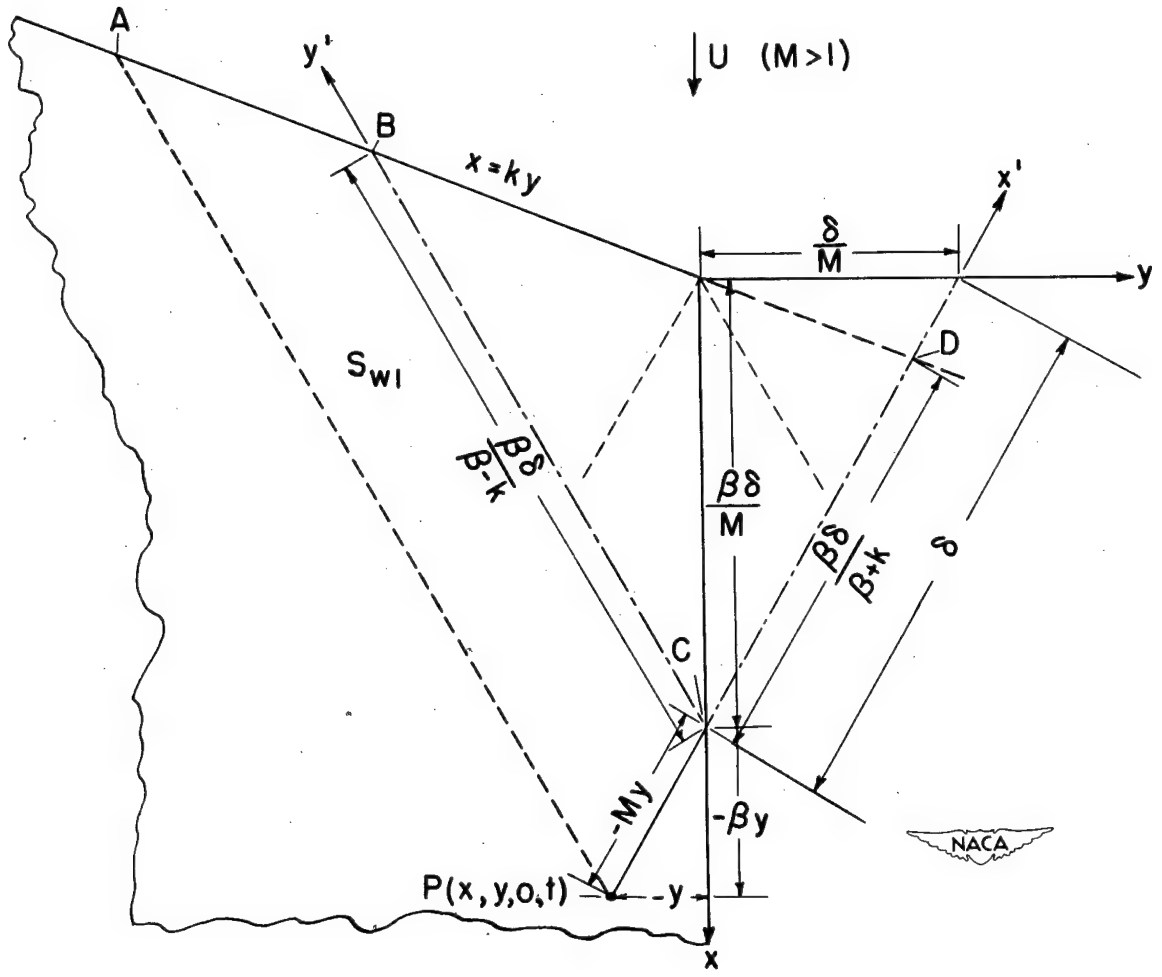

Figure 6.- Wing area S_{wl} (PABC) which affects the potential at P(x,y) and the oblique coordinate system (x',y') chosen for calculation in second method.

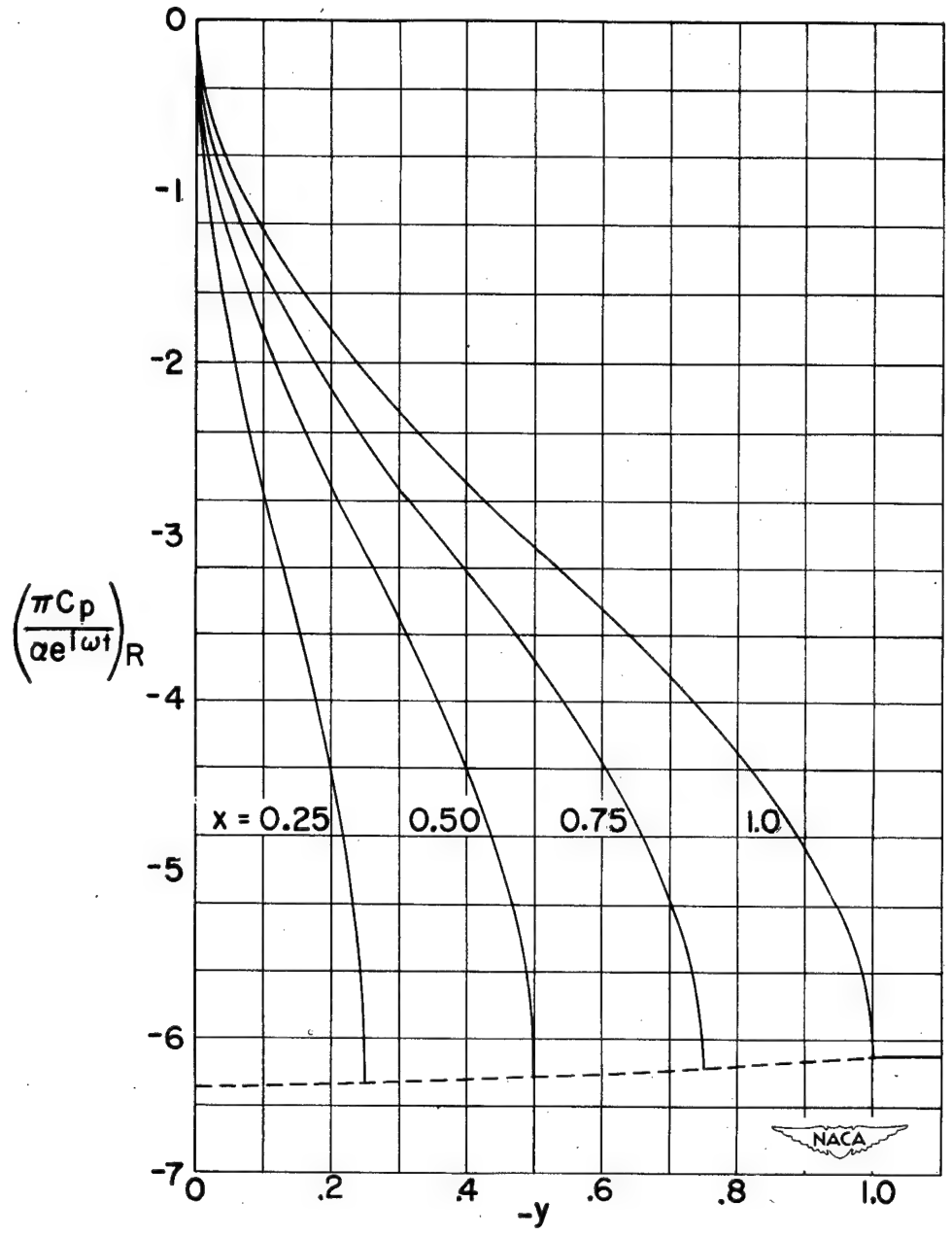

(a) Real part of $\frac{\pi C_p}{\alpha e^{i\omega t}}$.

Figure 7.- Real and imaginary parts of $\frac{\pi C_p}{\alpha e^{i\omega t}}$ along -y at various values of x for a rectangular wing tip (k = 0) of unit chord with $\frac{\omega c}{a} = 0.2$ and $M = \sqrt{2}$ (used for calculating pressure distribution on wing tip influenced by three-dimensional flow). Second method.

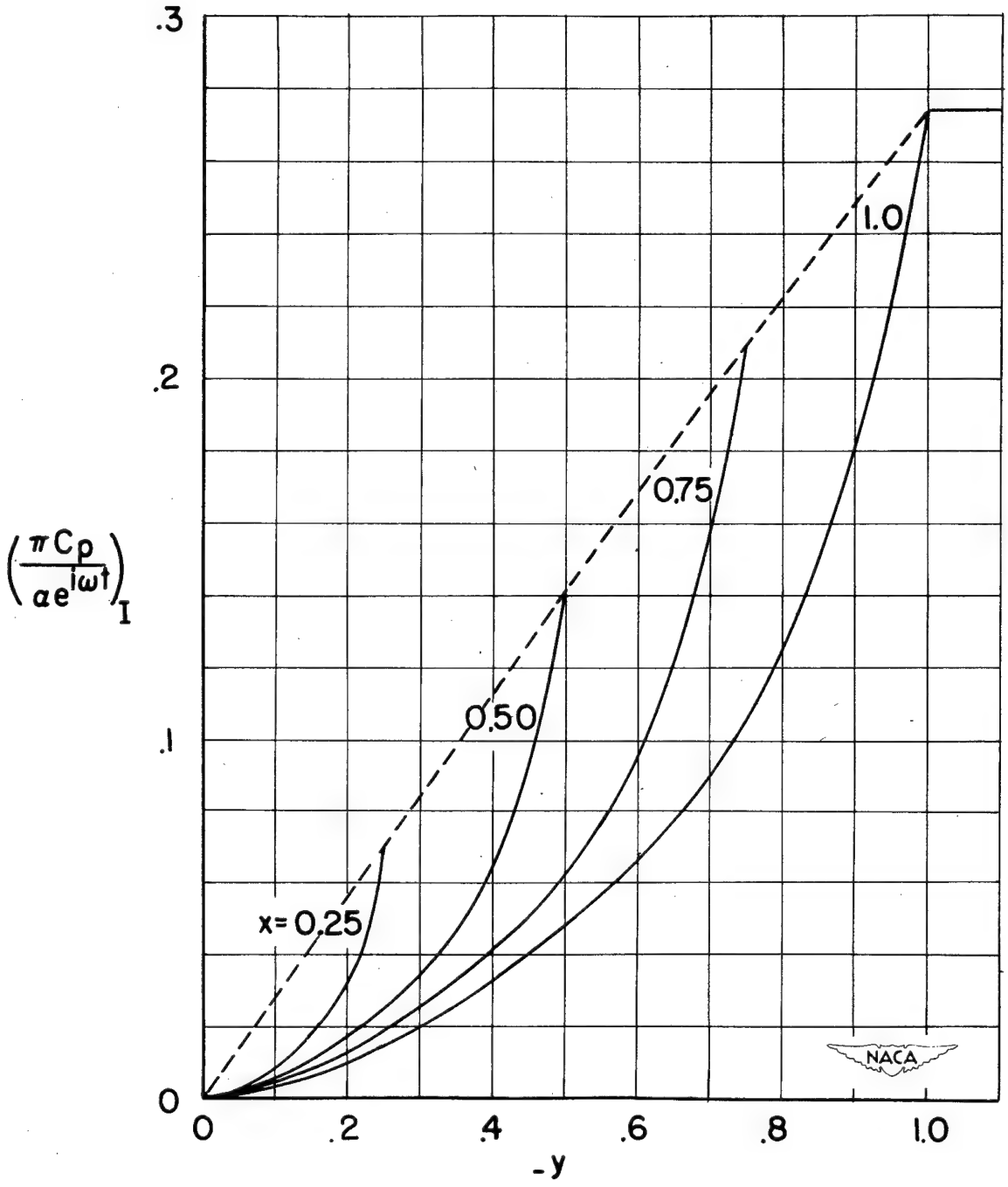

(b) Imaginary part of $\frac{\pi C_p}{\alpha e^{i\omega t}}$.

Figure 7.- Concluded.

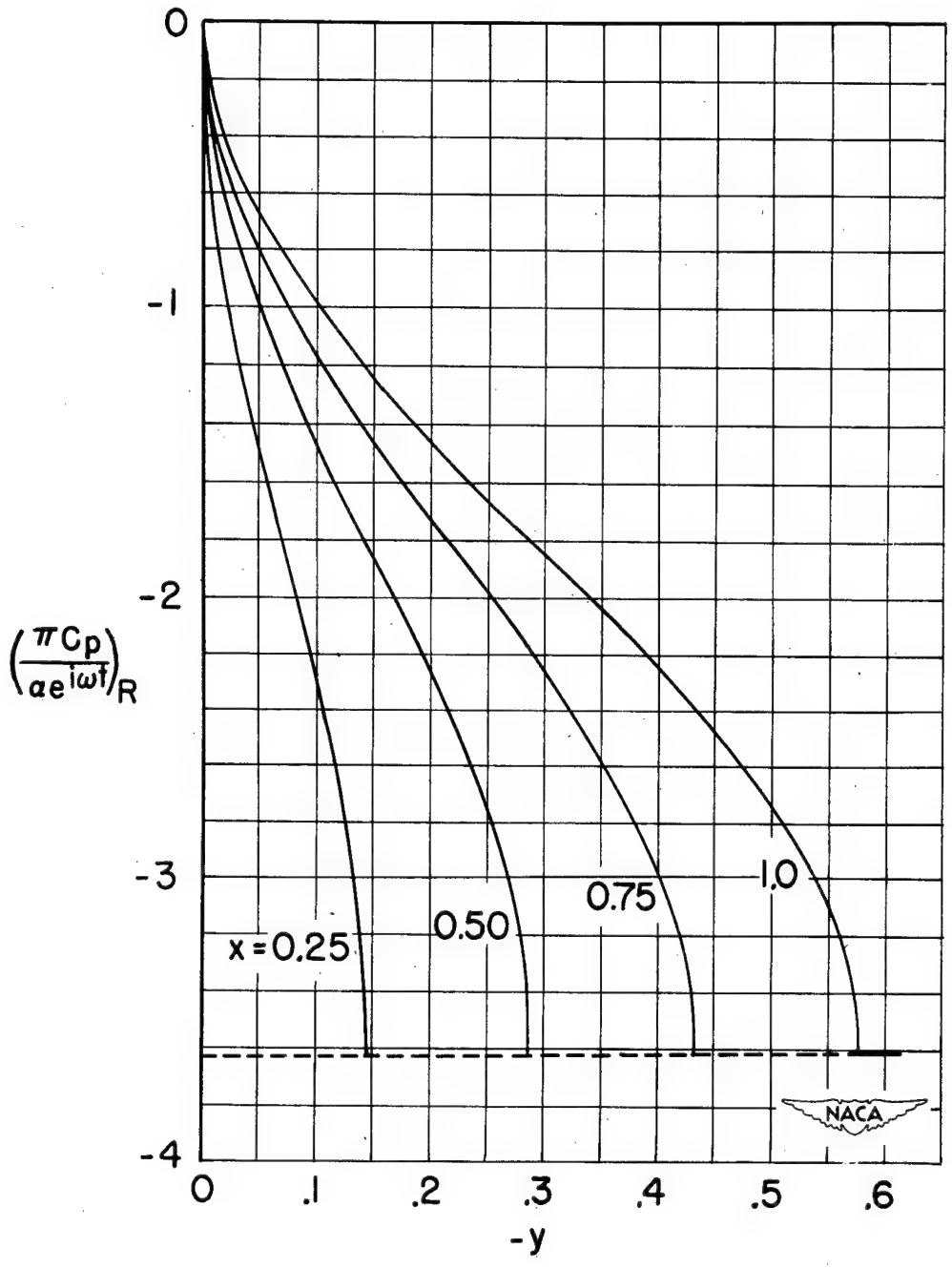

(a) Real part of $\frac{\pi C_p}{\alpha e^{i\omega t}}$.

Figure 8.- Real and imaginary parts of $\frac{\pi C_p}{\alpha e^{i\omega t}}$ along -y at various values of x for a rectangular wing tip (k = 0) of unit chord with $\frac{\omega c}{a}$ = 0.2 and M = 2.

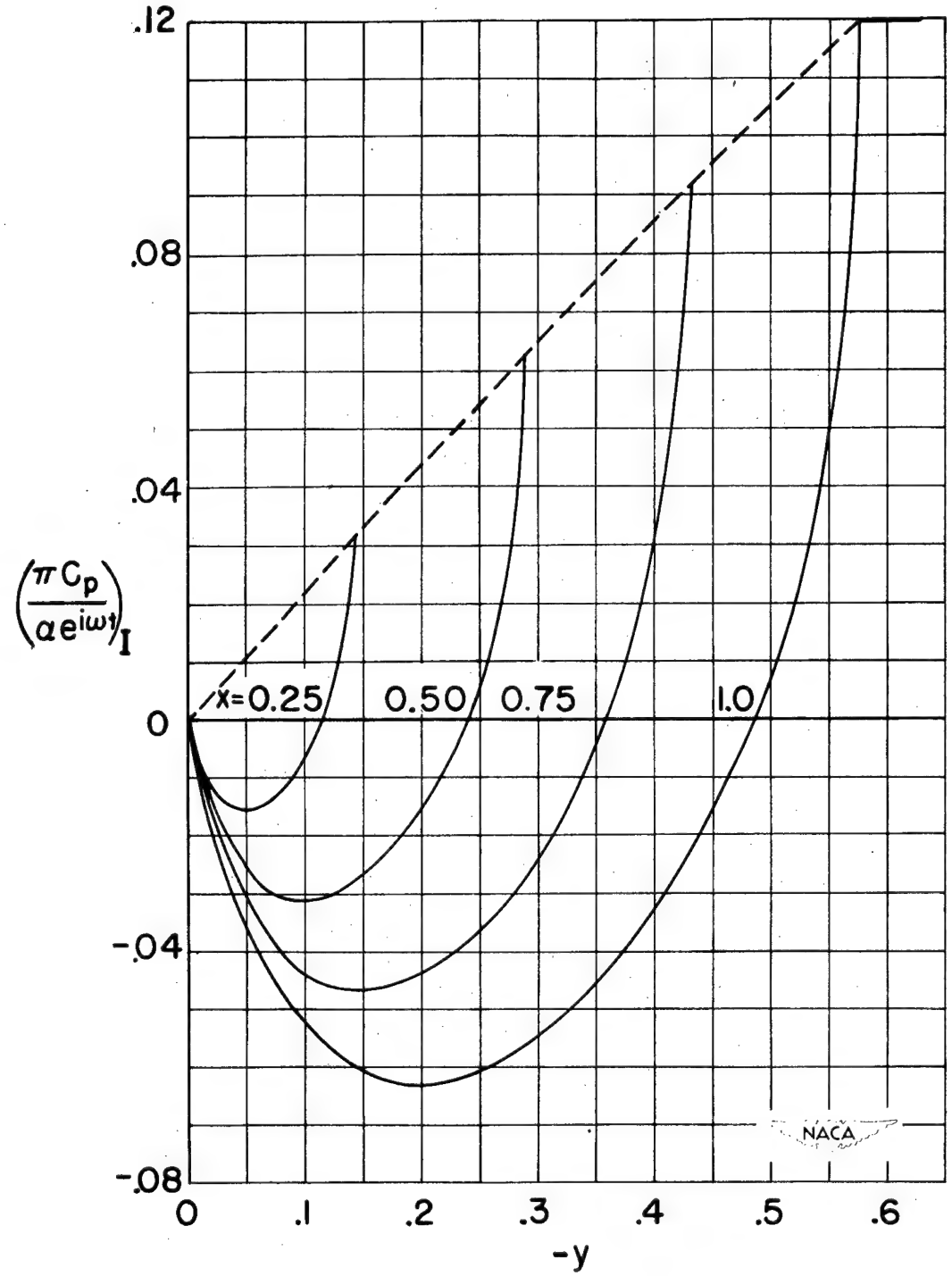

(b) Imaginary part of $\frac{\pi C_p}{\alpha e^{i\omega t}}$.

Figure 8.- Concluded.

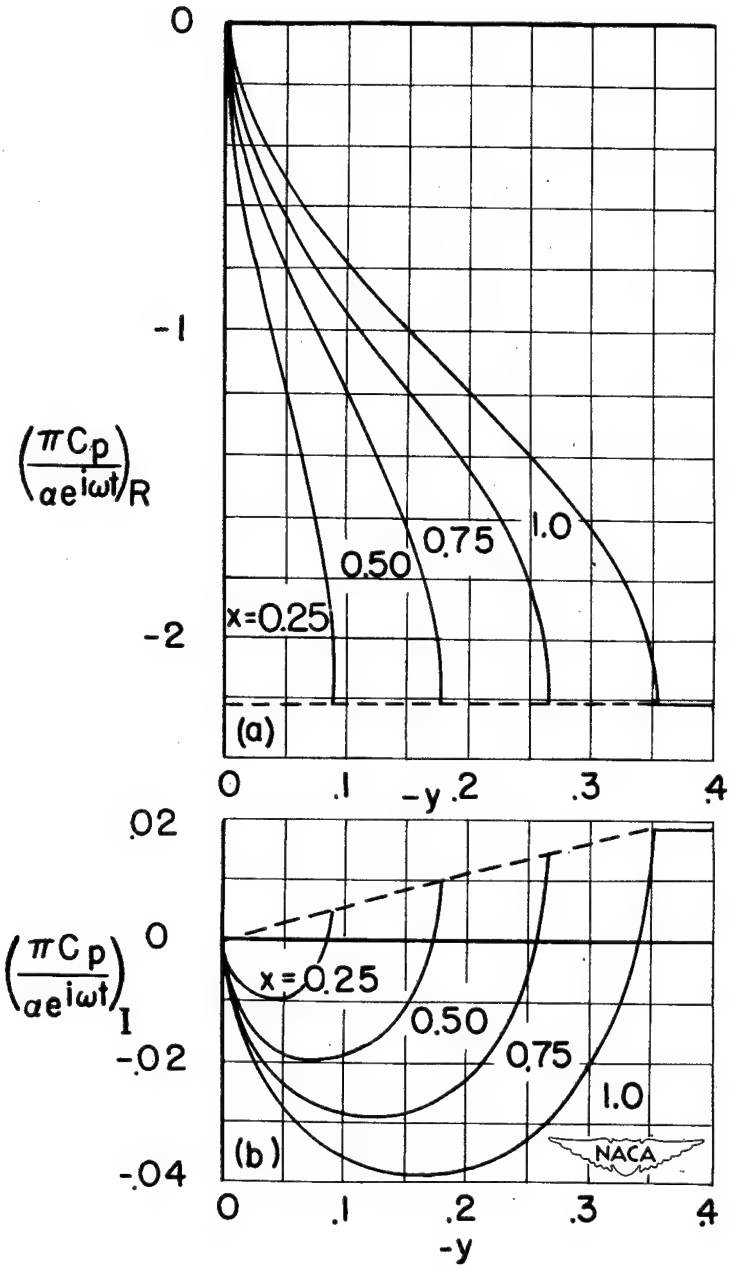

(a) Real part of $\frac{\pi C_p}{\alpha e^{i\omega t}}$.

(b) Imaginary part of $\frac{\pi C_p}{\alpha e^{i\omega t}}$.

Figure 9.- Real and imaginary parts of $\frac{\pi C_p}{\alpha e^{i\omega t}}$ along -y at various values of x for a rectangular wing tip (k = 0) of unit chord with $\frac{\omega c}{a}$ = 0.2 and M = 3.

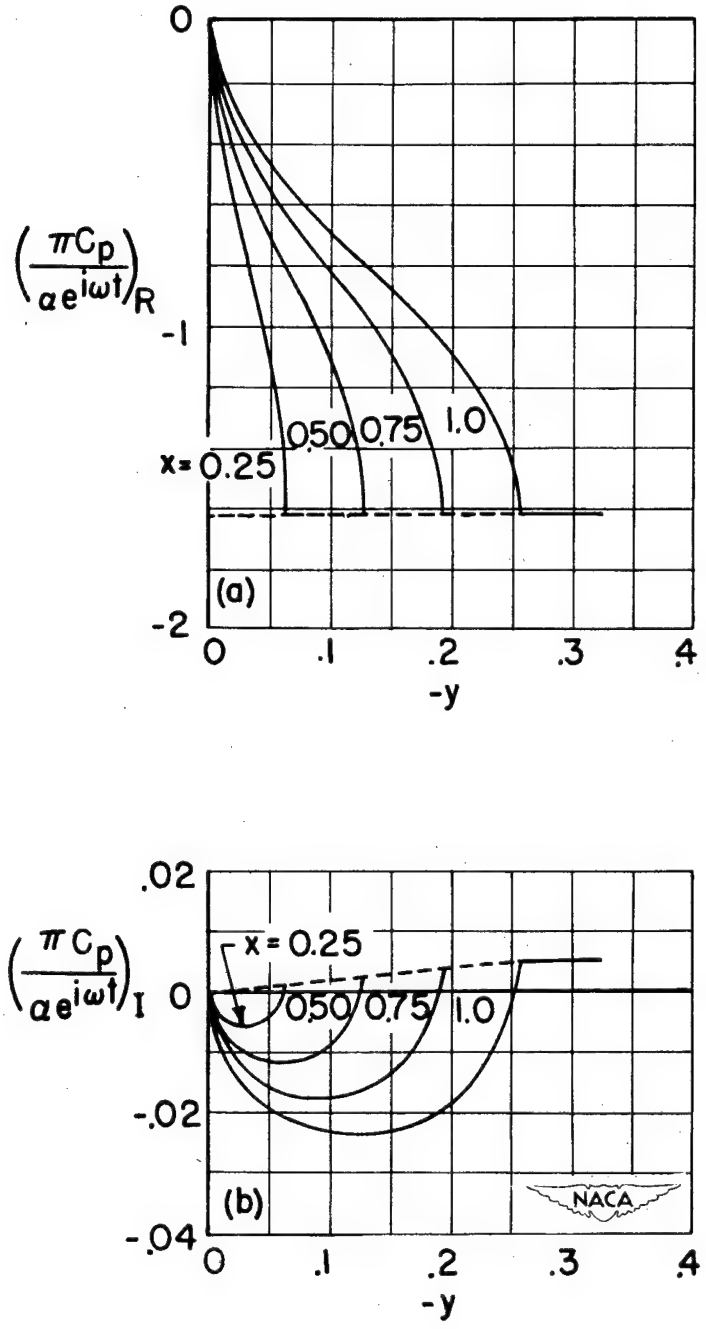

(a) Real part of $\frac{\pi C_p}{\alpha e^{i\omega t}}$.

(b) Imaginary part of $\frac{\pi C_p}{\alpha e^{i\omega t}}$.

Figure 10.- Real and imaginary parts of $\frac{\pi C_p}{\alpha e^{i\omega t}}$ along -y at various values of x for a rectangular wing tip (k = 0) of unit chord with $\frac{\omega c}{a} = 0.2$ and M = 4.

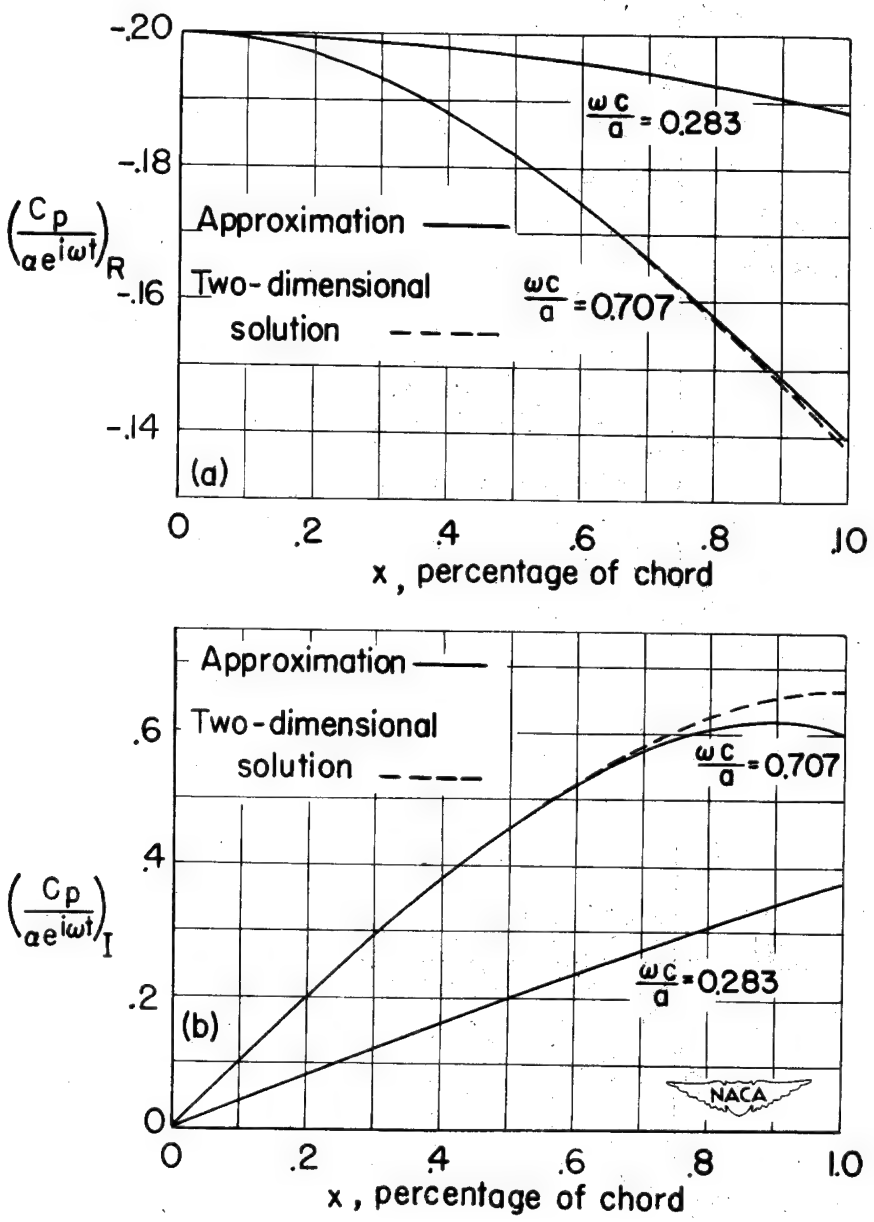

(a) Real part of $\frac{C_p}{\alpha e^{i\omega t}}$.

(b) Imaginary part of $\frac{C_p}{\alpha e^{i\omega t}}$.

Figure 11.- Comparison of results of second approximation with two-dimensional solutions at left tip Mach line of right rectangular wing tip (k = 0) along chord at $\frac{\omega c}{a\beta^2}$ = 0.283 and $\frac{\omega c}{a\beta^2}$ = 0.707 with M = $\sqrt{2}$.

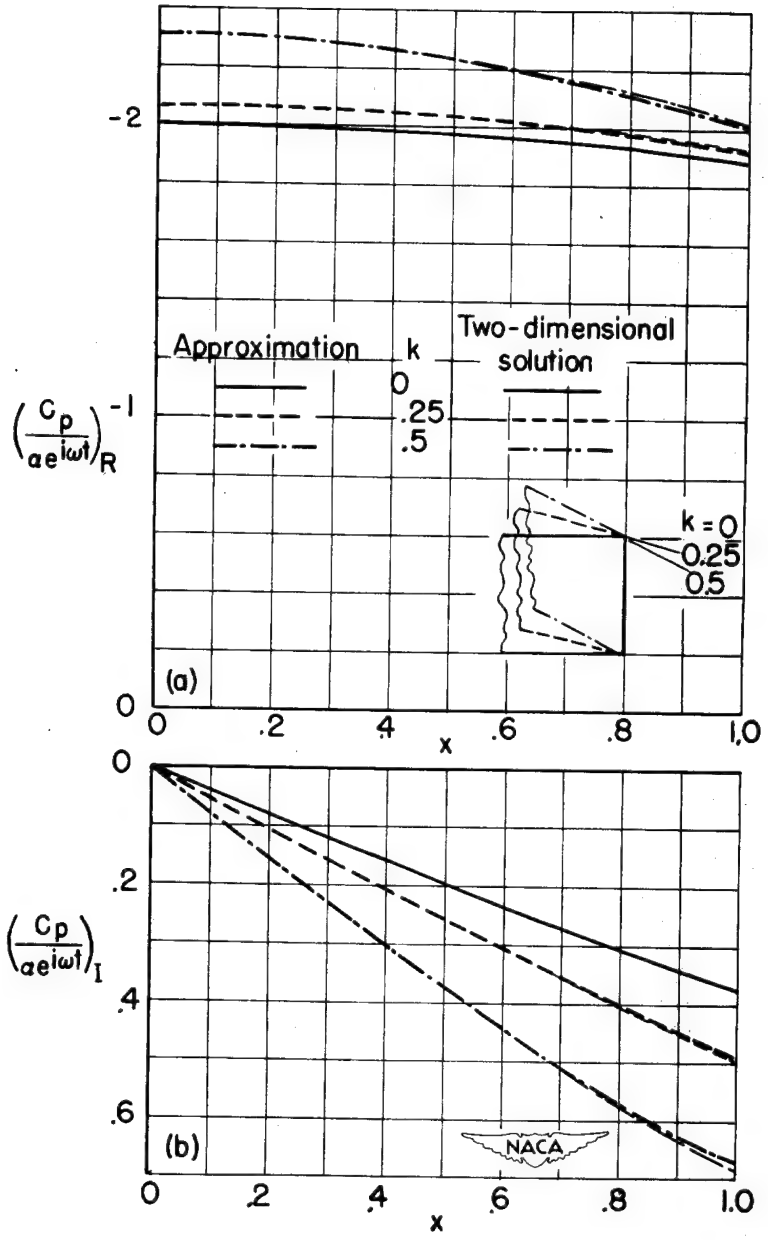

(a) Real part of $\frac{C_p}{\alpha e^{i\omega t}}$.

(b) Imaginary part of $\frac{C_p}{\alpha e^{i\omega t}}$.

Figure 12.- Comparisons of results of second approximation with two-dimensional solutions at left tip Mach line of a right sweptback wing tip along chord for various values of k. $k = \tan \Lambda = 0.25$ and 0.5, $\frac{\omega c}{a\beta^2} = 0.283$, and $M = \sqrt{2}$.

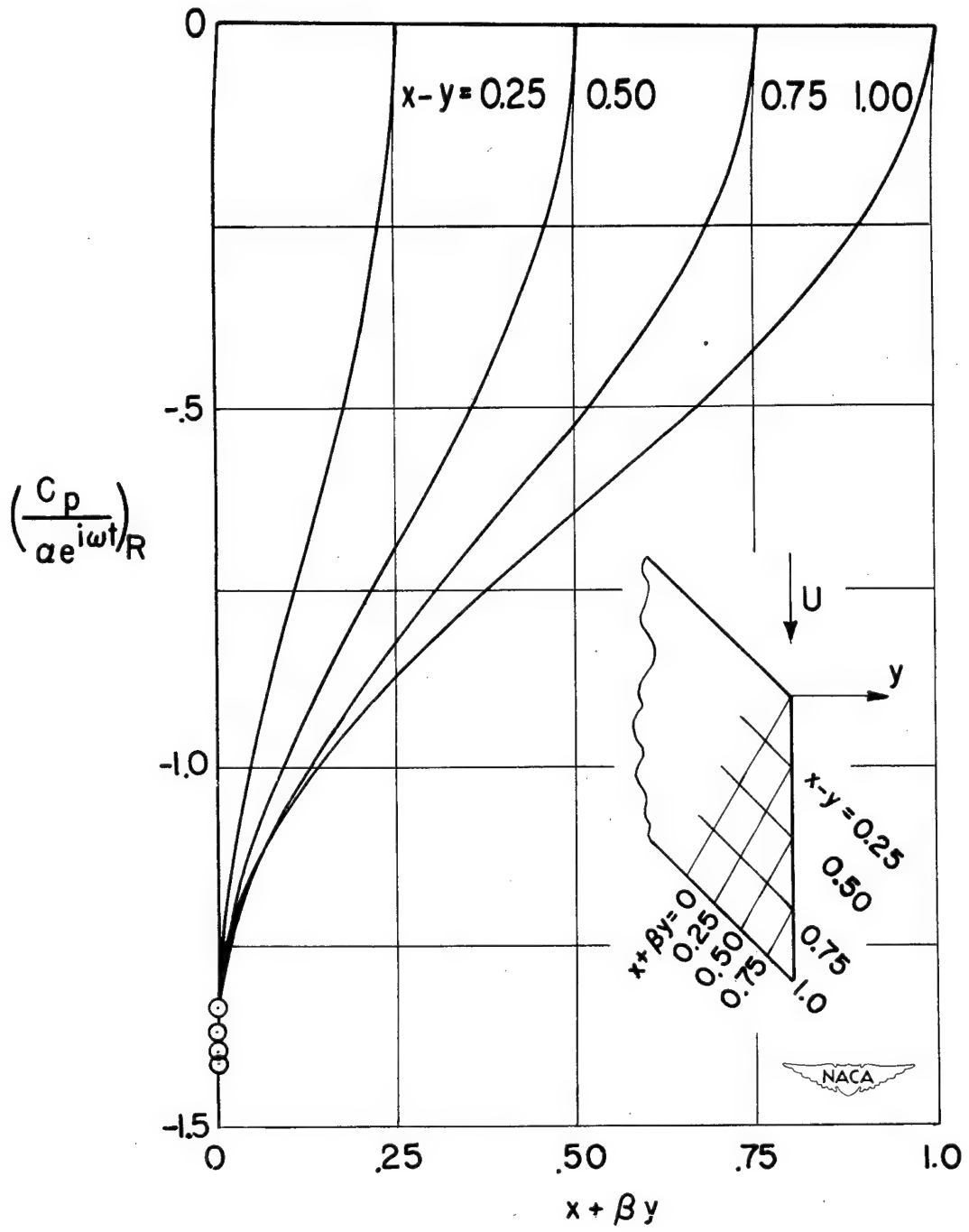

(a) Real part of $\frac{C_p}{\alpha e^{i\omega t}}$.

Figure 13.- Distribution of $\frac{C_p}{\alpha e^{i\omega t}}$ along constant $x - y$ at various values of $x + \beta y$ for a 45° sweptback wing tip at $M = 2$, $\frac{\omega c}{a} = 0.4$, and $k = 1$.

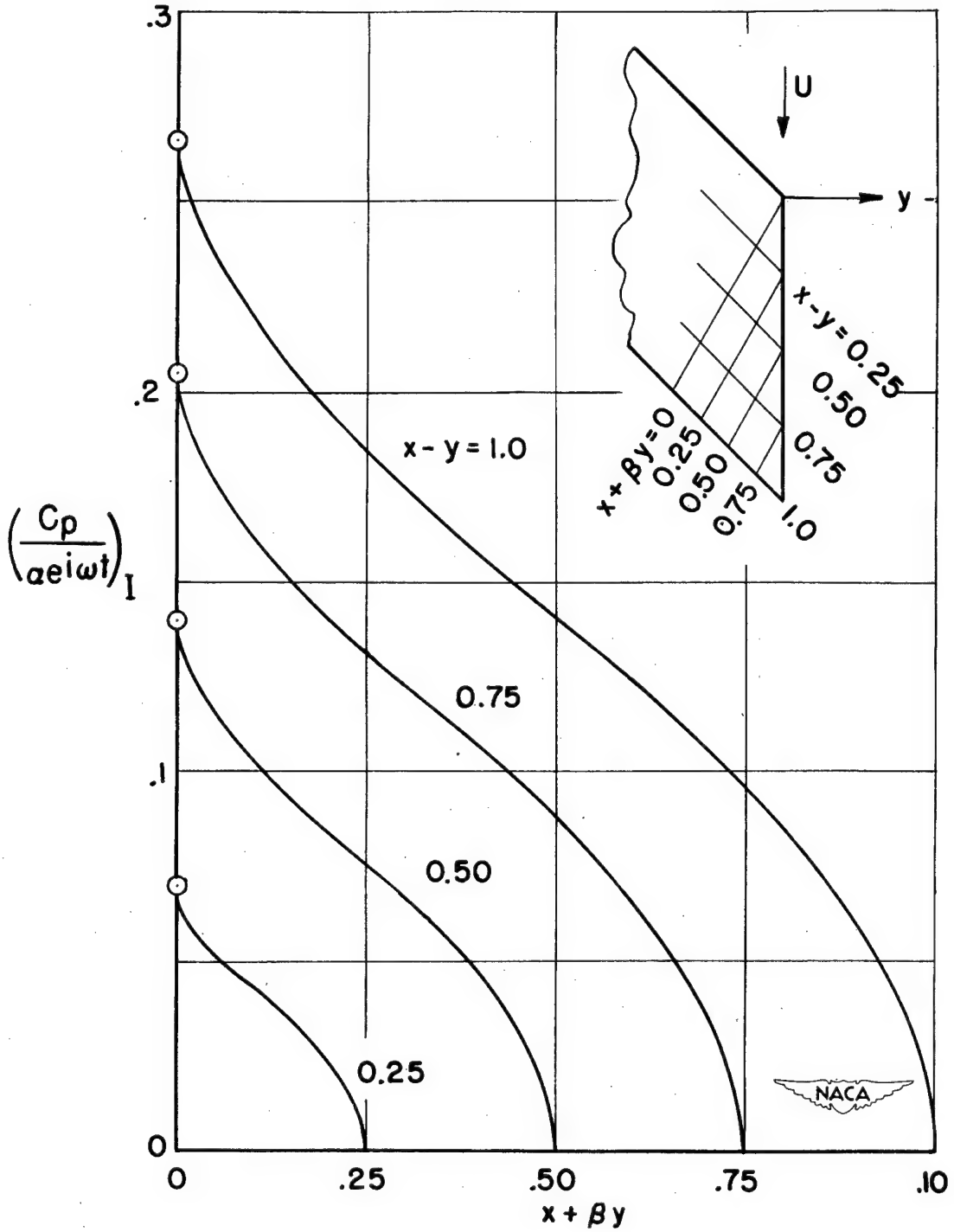

(b) Imaginary part of $\frac{C_p}{\alpha e^{i\omega t}}$.

Figure 13.- Concluded.

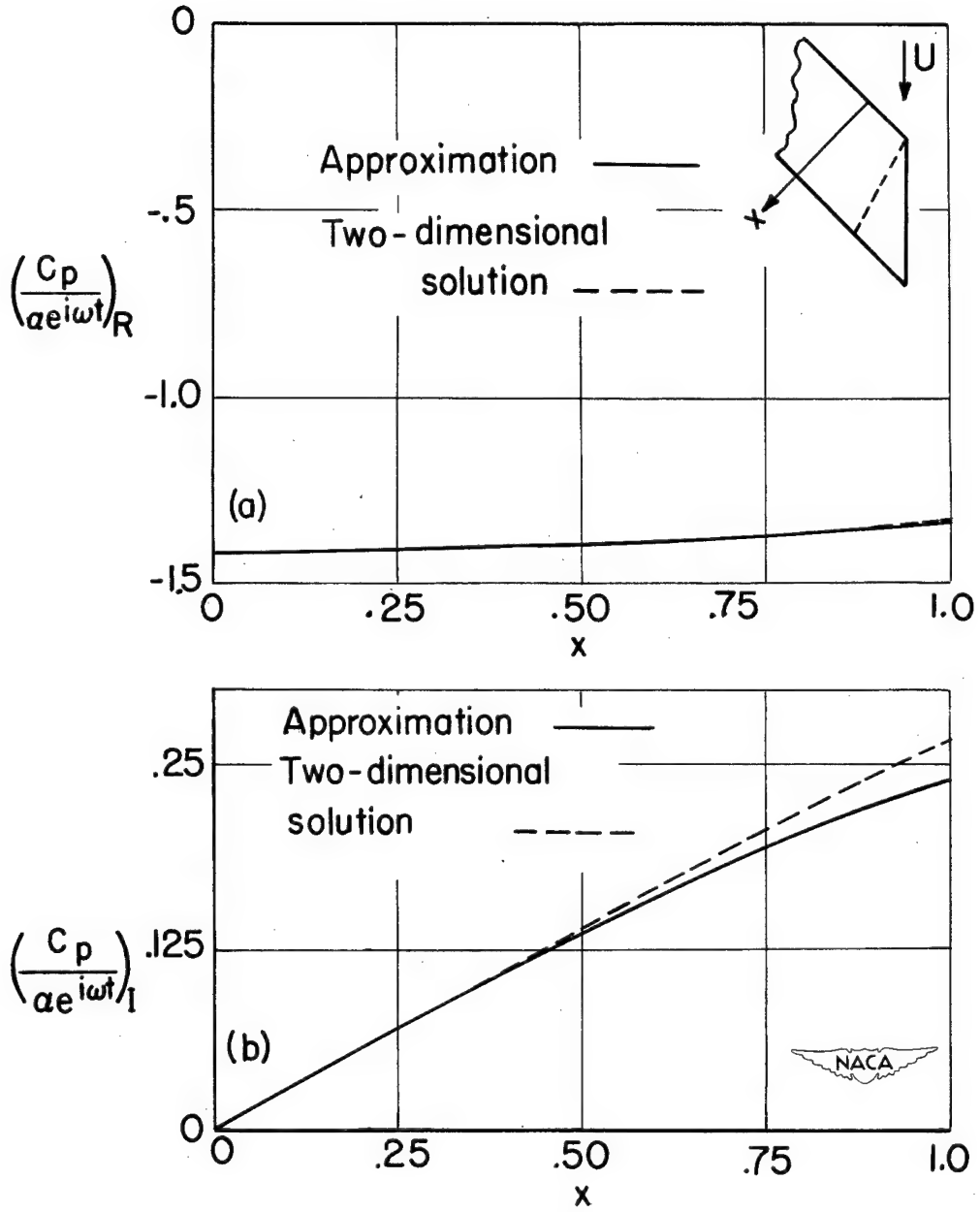

(a) Real part of $\frac{C_p}{\alpha e^{i\omega t}}$.

(b) Imaginary part of $\frac{C_p}{\alpha e^{i\omega t}}$.

Figure 14.- Comparison of results of second approximation with two-dimensional solutions at left tip Mach line of a sweptback wing tip along chord. Sweepback angle, 45°; M = 2; $\frac{\omega c}{a}$ = 0.4, k = 1.

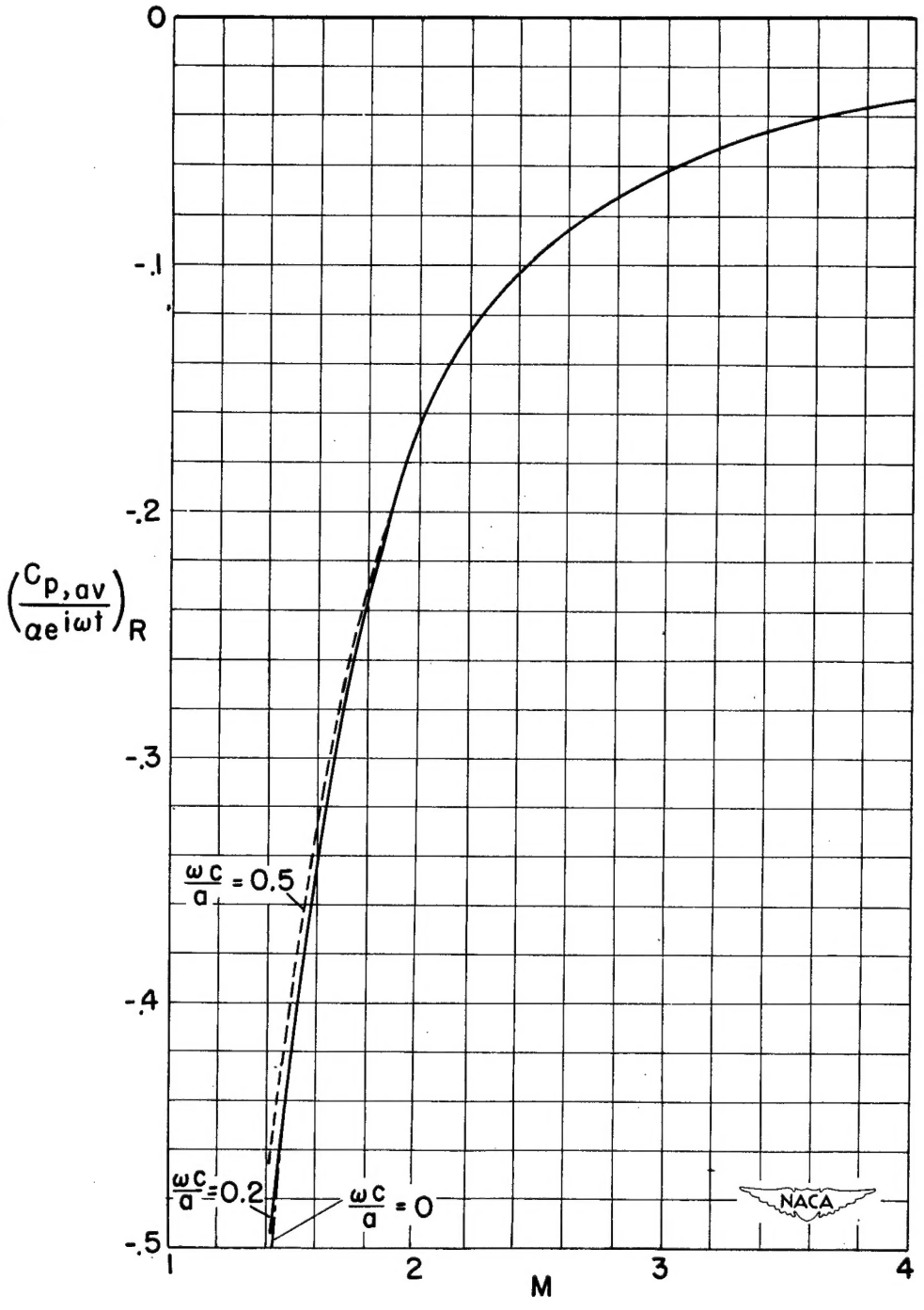

(a) Real part of $\frac{C_{p,av}}{\alpha e^{i\omega t}}$.

Figure 15.- Average pressure distribution over entire rectangular wing tip (k = 0) influenced by three-dimensional flow as it varies with Mach number for $\frac{\omega c}{a} = 0$, $\frac{\omega c}{a} = 0.2$, and $\frac{\omega c}{a} = 0.5$.

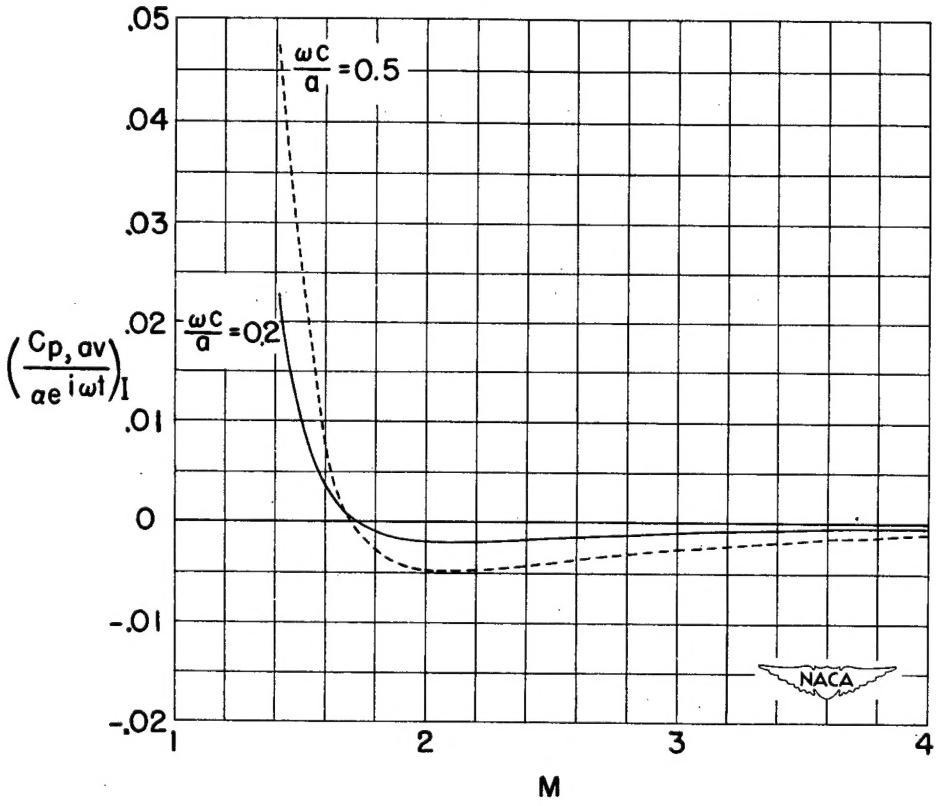

(b) Imaginary part of $\frac{C_{pa}}{\alpha e^{i\omega t}}$.

Figure 15.- Concluded.

NACA TN 2467
National Advisory Committee for Aeronautics.
THE AERODYNAMIC BEHAVIOR OF A HARMONICALLY OSCILLATING FINITE SWEPTBACK WING IN SUPERSONIC FLOW. Chieh-Chien Chang, Johns Hopkins University. October 1951. 76p. diagrs. (NACA TN 2467)

By an extension of Evvard's "diaphragm" concept outside the wing tip, two approximate methods are presented for calculating the aerodynamic behavior of harmonically oscillating, sweptback finite wings with both supersonic leading and trailing edges - one expressing the integration in terms of Fresnal integrals and the second one similar to the first except that a series expansion of the source-strength function is used. If the wing frequency parameter is small both methods give accurate results in the engineering sense without requiring undue computing skill. A number of graphs are presented to show pressure distribution of the wings at different Mach

Copies obtainable from NACA, Washington (over)

1. Flow, Supersonic (1.1.2.3)
2. Wings, Complete - Theory (1.2.2.1)
3. Wings, Complete - Sweep (1.2.2.2.3)
4. Vibration and Flutter - Wings and Ailerons (4.2.1)

I. Chang, Chieh-Chien
II. NACA TN 2467
III. Johns Hopkins U.

NACA TN 2467
National Advisory Committee for Aeronautics.
THE AERODYNAMIC BEHAVIOR OF A HARMONICALLY OSCILLATING FINITE SWEPTBACK WING IN SUPERSONIC FLOW. Chieh-Chien Chang, Johns Hopkins University. October 1951. 76p. diagrs. (NACA TN 2467)

By an extension of Evvard's "diaphragm" concept outside the wing tip, two approximate methods are presented for calculating the aerodynamic behavior of harmonically oscillating, sweptback finite wings with both supersonic leading and trailing edges - one expressing the integration in terms of Fresnal integrals and the second one similar to the first except that a series expansion of the source-strength function is used. If the wing frequency parameter is small both methods give accurate results in the engineering sense without requiring undue computing skill. A number of graphs are presented to show pressure distribution of the wings at different Mach

Copies obtainable from NACA, Washington (over)

1. Flow, Supersonic (1.1.2.3)
2. Wings, Complete - Theory (1.2.2.1)
3. Wings, Complete - Sweep (1.2.2.2.3)
4. Vibration and Flutter - Wings and Ailerons (4.2.1)

I. Chang, Chieh-Chien
II. NACA TN 2467
III. Johns Hopkins U.

NACA TN 2467
National Advisory Committee for Aeronautics.
THE AERODYNAMIC BEHAVIOR OF A HARMONICALLY OSCILLATING FINITE SWEPTBACK WING IN SUPERSONIC FLOW. Chieh-Chien Chang, Johns Hopkins University. October 1951. 76p. diagrs. (NACA TN 2467)

By an extension of Evvard's "diaphragm" concept outside the wing tip, two approximate methods are presented for calculating the aerodynamic behavior of harmonically oscillating, sweptback finite wings with both supersonic leading and trailing edges - one expressing the integration in terms of Fresnal integrals and the second one similar to the first except that a series expansion of the source-strength function is used. If the wing frequency parameter is small both methods give accurate results in the engineering sense without requiring undue computing skill. A number of graphs are presented to show pressure distribution of the wings at different Mach

Copies obtainable from NACA, Washington (over)

1. Flow, Supersonic (1.1.2.3)
2. Wings, Complete - Theory (1.2.2.1)
3. Wings, Complete - Sweep (1.2.2.2.3)
4. Vibration and Flutter - Wings and Ailerons (4.2.1)

I. Chang, Chieh-Chien
II. NACA TN 2467
III. Johns Hopkins U.

NACA TN 2467
National Advisory Committee for Aeronautics.
THE AERODYNAMIC BEHAVIOR OF A HARMONICALLY OSCILLATING FINITE SWEPTBACK WING IN SUPERSONIC FLOW. Chieh-Chien Chang, Johns Hopkins University. October 1951. 76p. diagrs. (NACA TN 2467)

By an extension of Evvard's "diaphragm" concept outside the wing tip, two approximate methods are presented for calculating the aerodynamic behavior of harmonically oscillating, sweptback finite wings with both supersonic leading and trailing edges - one expressing the integration in terms of Fresnal integrals and the second one similar to the first except that a series expansion of the source-strength function is used. If the wing frequency parameter is small both methods give accurate results in the engineering sense without requiring undue computing skill. A number of graphs are presented to show pressure distribution of the wings at different Mach

Copies obtainable from NACA, Washington (over)

1. Flow, Supersonic (1.1.2.3)
2. Wings, Complete - Theory (1.2.2.1)
3. Wings, Complete - Sweep (1.2.2.2.3)
4. Vibration and Flutter - Wings and Ailerons (4.2.1)

I. Chang, Chieh-Chien
II. NACA TN 2467
III. Johns Hopkins U.

NACA TN 2467

numbers, sweepback angles, and frequency parameters. Comparisons of pressure coefficients calculated from present methods and exact two dimensional solutions based on linearized theory are made.

Copies obtainable from NACA, Washington

NACA TN 2467

numbers, sweepback angles, and frequency parameters. Comparisons of pressure coefficients calculated from present methods and exact two dimensional solutions based on linearized theory are made.

Copies obtainable from NACA, Washington

NACA TN 2467

numbers, sweepback angles, and frequency parameters. Comparisons of pressure coefficients calculated from present methods and exact two dimensional solutions based on linearized theory are made.

Copies obtainable from NACA, Washington

NACA TN 2467

numbers, sweepback angles, and frequency parameters. Comparisons of pressure coefficients calculated from present methods and exact two dimensional solutions based on linearized theory are made.

Copies obtainable from NACA, Washington